

State of Oregon
Department of Geology and Mineral Industries
Vicki S. McConnell, State Geologist

GEOLOGIC MAP SERIES
GMS-119

**GEOLOGIC MAP OF THE OREGON CITY 7.5' QUADRANGLE,
CLACKAMAS COUNTY, OREGON**

By
Ian P. Madin

Oregon Department of Geology and Mineral Industries
800 NE Oregon Street #28, Suite 965, Portland, OR 97232
email: ian.madin@dogami.state.or.us



2009

NOTICE

The Oregon Department of Geology and Mineral Industries is publishing this map because the subject matter is consistent with the mission of the Department. The map is not intended to be used for site-specific planning. The map cannot serve as a substitute for site-specific investigations by qualified practitioners. Site-specific data may give results that differ from those shown on the map. The views and conclusions contained in this document are those of the author and should not be interpreted as necessarily representing the official policies, either expressed or implied, of the U.S. Government.

Oregon Department of Geology and Mineral Industries Geologic Map 119
Published in conformance with ORS 516.030

For copies of this publication or other information about Oregon's geology and natural resources, contact:

Nature of the Northwest Information Center
800 NE Oregon Street #28, Suite 965
Portland, Oregon 97232
(971) 673-1555
<http://www.naturenw.org>

For additional information:
Administrative Offices
800 NE Oregon Street #28, Suite 965
Portland, OR 97232
Telephone (971) 673-1555
Fax (971) 673-1562
<http://www.oregongeology.com>
<http://egov.oregon.gov/DOGAMI/>

TABLE OF CONTENTS

INTRODUCTION	1
Previous work	1
METHODS	3
DESCRIPTION OF UNITS	4
Quaternary Surficial Deposits	4
Boring Volcanic Field Rocks	8
Miocene-Pleistocene Fluvial Sedimentary Rocks	23
Columbia River Basalt Group	30
Wanapum Basalt-Frenchman Springs Member	30
Grande Ronde Basalt	32
STRUCTURE	36
Bolton Fault	36
Portland Hills Fault	38
Oatfield (?) Fault	38
Minor Faults	38
RESOURCES	39
HAZARDS	43
GEOLOGIC HISTORY	43
ACKNOWLEDGMENTS	44
REFERENCES	45

All appendices are in digital format only; they can be found on the CD-ROM of this publication.

APPENDIX A: FIELD STATIONS

APPENDIX B: WELL DATA

APPENDIX C: SCANNED IMAGES OF PETROGRAPHIC THIN SECTIONS

APPENDIX D: GEOCHEMICAL DATA

APPENDIX E: FIELD PHOTOGRAPHS

APPENDIX F: COLUMBIA RIVER BASALT WELL DATA

LIST OF FIGURES

Figure 1. Shaded relief map of the Portland, Oregon, urban area, showing study location	1
Figure 2. Orthophoto image showing development patterns in the Oregon City, Oregon, quadrangle	2
Figure 3. Debris flow-earthflow fans visible in lidar digital elevation model.	4
Figure 4. Outcrop, Missoula (Bretz) flood deposits	6
Figure 5. Landslide graben.	7
Figure 6. Landslide features visible in lidar DEM	7
Figure 7. Hand specimen, basaltic andesite of Outlook.	8
Figure 8. Petrography, basaltic andesite of Outlook	8
Figure 9. Boring volcanic field lava composition	9
Figure 10. Cr versus Sr plot of Boring volcanic field rocks	9
Figure 11. Volcanic vents, Boring Lava	10
Figure 12. Hand specimen, basaltic andesite of Hunsinger	11
Figure 13. Quarry outcrop, basaltic andesite of Hunsinger	11
Figure 14. Petrography, basaltic andesite of Hunsinger	12
Figure 15. Hand specimen, basalt of Canemah	13
Figure 16. Jointing, basalt of Canemah	13
Figure 17. Weathering, basalt of Canemah	14

(List of Figures, continued)

Figure 18. Petrography, basalt of Canemah	14
Figure 19. Basal contact, basalt of Canemah	14
Figure 20. Basalt contact surface data	15
Figure 21. Lava tube, basalt of Canemah.	15
Figure 22. Isopach map, basalt of Canemah.	17
Figure 23. Hand specimen, basaltic andesite of Root Creek	17
Figure 24. Basaltic andesite of Root Creek	18
Figure 25. Petrography , basaltic andesite of Root Creek.	18
Figure 26. Hand specimen, basalt of Fallsview	20
Figure 27. Petrography, basalt of Fallsview	20
Figure 28. Basalt of Fallsview vent	20
Figure 29. Fallsview tephra	22
Figure 30. Hand specimen, basaltic andesite of Beaver Creek	22
Figure 31. Basaltic andesite of Beaver Creek	22
Figure 32. Petrography, basaltic andesite of Beaver Creek.	22
Figure 33. Springwater Formation conglomerate	24
Figure 34. Troutdale Formation facies	25
Figure 35. Hand specimens, Troutdale Formation mudstone	26
Figure 36. Petrography, Troutdale Formation mudstone.	26
Figure 37. Petrography, Troutdale Formation mudstone.	26
Figure 38. Outcrop, Troutdale Formation laminated mudstone	26
Figure 39. Outcrop, Troutdale Formation massive mudstone	27
Figure 40. Hand specimens, Troutdale Formation sandstone	27
Figure 41. Petrography, Troutdale Formation micaceous quartzo-feldspathic sandstone	27
Figure 42. Petrography, Troutdale Formation volcanic-lithic sandstone	27
Figure 43. Outcrop, Troutdale Formation volcanic lithic sandstone	28
Figure 44. Petrography, Troutdale Formation conglomerate	28
Figure 45. Petrography, Troutdale Formation conglomerate	28
Figure 46. Outcrop, Troutdale Formation conglomerate.. . . .	29
Figure 47. Hand specimen, basalt of Sand Hollow.	31
Figure 48. Petrography, basalt of Sand Hollow	31
Figure 49. Columbia River Basalt Group lava composition.	31
Figure 50. Columbia River Basalt Group Ti versus Cr plot.	31
Figure 51. Hand specimen, basalt of Gingko	33
Figure 52. Outcrops, basalt of Gingko.	33
Figure 53. Petrography, basalt of Gingko.	33
Figure 54. Hand specimen, Sentinel Bluffs Member of Grande Ronde Basalt	34
Figure 55. Outcrops, Sentinel Bluffs Member of Grande Ronde Basalt	34
Figure 56. Hand specimen, Vantage Member sandstone of the Ellensburg Formation	34
Figure 57. Willamette Falls and Sentinel Bluffs member of the Grande Ronde Basalt.	35
Figure 58. Regional landforms and structures in the vicinity of the Oregon City quadrangle.	37
Figure 59. Horizontally offset (?) valley-filling flow of the basaltic andesite of Beaver Creek	38
Figure 60. Lidar image of area of inferred trace of the Bolton Fault.. . . .	38
Figure 61. Well yield data in the Oregon City quadrangle	40
Figure 62. Reported depth to first water in the Oregon City quadrangle	41
Figure 63. Static water level in the Oregon City quadrangle	42

MAP PLATE

Plate 1. Geologic map of the Oregon City 7.5' quadrangle, Clackamas County, Oregon, scale 1:24,000

INTRODUCTION

The Oregon City 7.5' quadrangle is located in the south of the Portland urban area in northwestern Oregon (Figure 1). Topographically, most of the area is a gently rolling plateau ranging from about 120 m to 210 m in elevation. In the northwest corner of the quadrangle the plateau is cut by the canyon of the Willamette River, which is near sea level in elevation. The plateau is also cut by the canyon of Abernethy Creek, which cuts across the northeast part of the map, and by the canyon of Beaver Creek, which cuts west to east across the center of the quadrangle. The northwest corner of the map area is heavily urbanized and includes the cities of West Linn and Oregon City, which was founded in 1829 to exploit water power at Willamette Falls. The remainder of the quadrangle is a mix of small farms and woodlots and rural residential development (Figure 2). At the time of field work, denser residential development was spreading south from Oregon City.

This map was prepared as part of a 5-year collaborative effort between the U.S. Geological Survey (USGS) and the Oregon Department of Geology and Mineral Industries (DOGAMI) to improve geologic mapping in the Portland urban area in order to better understand earthquake hazards. The Oregon City quadrangle was chosen because two major faults, the Bolton Fault and Portland Hills Fault, project into the map area from the northwest. Where mapped to the northwest, these faults are known to cut only Miocene rocks, and traverse only Miocene or latest Quaternary deposits (Beeson and others, 1989). In the Oregon City quadrangle, a thick section of Pliocene to Pleistocene sedimentary and volcanic rocks provides the opportunity to refine the history of movement of these two faults. In addition, the detailed geologic mapping provides information about landslide hazards and groundwater resources in this rapidly developing area.

Previous work

Several previous geologic maps cover all or part of the study area. The earliest complete geologic map of the area was by Trimble (1963), at a scale of 1:125,000. The area was subsequently mapped, primarily for hazards, by Schlicker and Finlayson (1979) at a scale of 1:24,000; the geologic units in this study are largely derived from Trimble's earlier work. The adjacent Lake Oswego quadrangle was mapped at a scale of 1:24,000 (Beeson and others, 1989), as were the Gladstone quadrangle (Madin, 1990), Redland quadrangle (Madin, 2004), Damascus quadrangle (Madin, 1994), and Canby quadrangle (Beeson and Tolan, manuscript in preparation).

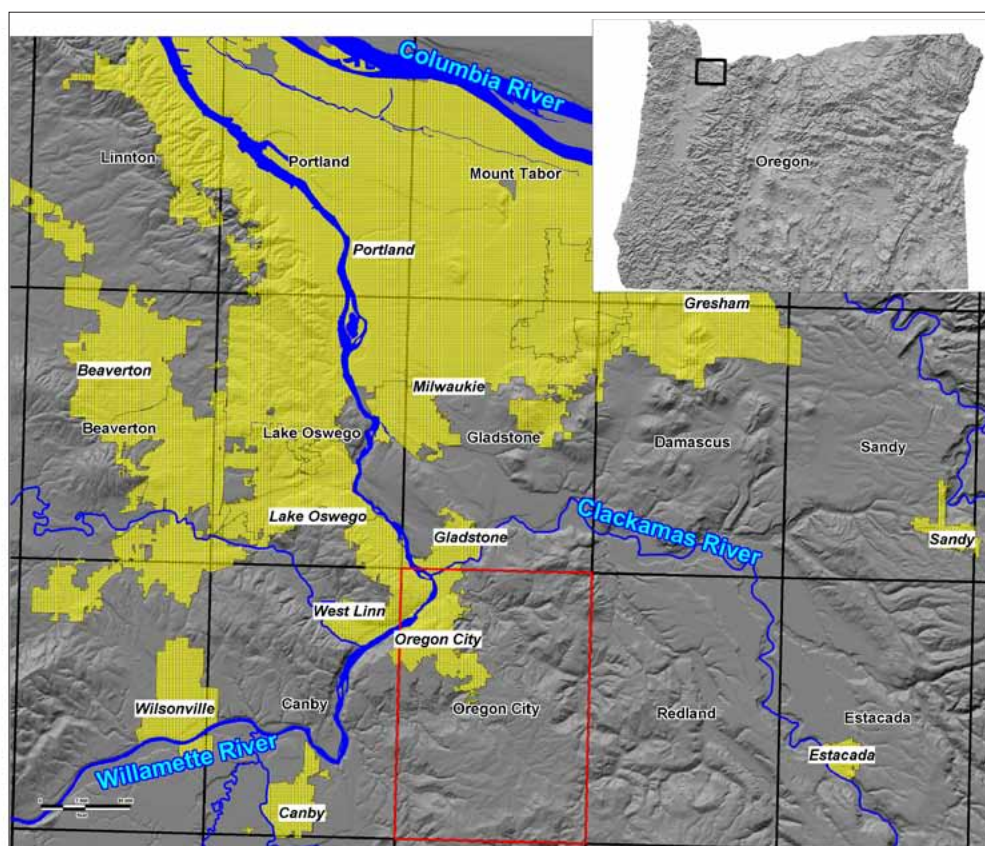


Figure 1. Shaded relief map of the Portland, Oregon, urban area in northwestern Oregon. Grid outlines 7.5' quadrangles, labeled with quadrangle name; study area is outlined in red. Yellow shading indicates area cities; selected cities are labeled in italics.



Figure 2. Orthophoto image showing development patterns in the Oregon City, Oregon, quadrangle. White lines are 7.5' quadrangle boundaries with adjacent quadrangles labeled; other labels are local road names. Base map is 2005 aerial imagery over lidar hillshade, scale 1:62,000.

METHODS

The geologic map was prepared using a variety of data sources that were digitally integrated with MapInfo™ geographical information system (GIS) software. The primary sources of data were field observations (see data map, Plate 1) in natural and man-made exposures. Over 600 observations were recorded digitally in the field using a Fujitsu Pen-centra™ tablet computer running ESRI Arcpad™ software. The field observations were located using a global positioning system (GPS) unit linked to the Penceutra, which allowed display of the GPS location on an image of the 7.5' topographic quadrangle map, allowing easy confirmation of the GPS position. The field data records for this project are included in digital format as Appendix A. The second major source of data was the logs of almost 1,300 approximately located water and engineering borings (see data map, Plate 1). Borings were located by comparing owner, tax lot, and address information on digital images of logs (available online through the Oregon Water Resources Department) with ownership, address, and tax lot information contained in the digital tax lot database for the area. Horizontal and vertical location errors were estimated for each located well, and the complete well database is included digitally as Appendix B. A limited number of wells were located in the field with GPS; for the remainder no field check was performed.

Several wells in the map area were analyzed geochemically and interpreted (USGS, 2006) by Marvin Beeson and Terry Tolan. Data from these wells were used in the preparation of the maps, and the interpreted logs are included as Appendix F.

The entire quadrangle was covered by high-resolution bare-earth lidar data obtained by the City of Oregon City in 2004 and by the Portland Lidar Consortium in 2007. Lidar-derived DEMs and contour maps provide a high-res-

olution, high-accuracy view of the true shape of the ground surface and were used to help interpret the geomorphology of the area. Lidar data were critical for mapping landslides and were very useful for accurate mapping of alluvial and terrace deposits. The field and boring data were integrated through analysis of lidar-derived digital elevation models (DEMs) and stereo air photos. Air photos were also used to map landslides that typically occur on steep, forested slopes of canyons. To see landslides in these situations, a time series (1939, 1948, 1956, 1964, 1973, 1980, 1990, 2000) of stereo air photos was examined. Additional landslide data were derived from a detailed study of part of Newell Canyon by Burns (1999).

Analytical data included petrographic thin sections of 28 samples, scanned images of which are provided in Appendix C. Sample numbers in the text correspond to field station numbers and locations in Appendix A. In addition, whole-rock major and trace element geochemical analyses of approximately 100 samples of Boring Lava and Columbia River basalt were used to help define volcanic units. Many of the data were made available by Richard Conrey (Washington State University) and Russell Evarts (USGS). The remaining samples were collected by the author and were analyzed by Stanley A. Mertzman of Franklin and Marshall College, Lancaster, Pennsylvania. Mertzman's methods are described in Appendix D; Conrey's methods are described by Johnson and others (1999). A few of the older analyses were performed by XRAL Laboratories, Don Mills, Ontario, Canada, in the early 1990s; there is no description of methods. Geochemical data are presented in Appendix D. Digital photographs associated with the field observations are also included as Appendix E, labeled with the station number of the corresponding field entry in Appendix A.

DESCRIPTION OF UNITS

af artificial fill (Recent)—man-made deposits of mixed clay, silt, sand, gravel, debris, and rubble. Includes large highway and freeway embankments and a major landfill southeast of the confluence of the Clackamas and Willamette rivers as well as numerous culvert fills and small dams. Mapped largely by interpretation of the lidar-derived DEM.

Quaternary Surficial Deposits

Qal alluvial deposits (Holocene)—gravel, sand, silt, and clay deposited in the active channels and floodplains of rivers and streams. In the Willamette and Clackamas rivers, alluvium is predominantly cobble gravel in both the channels and floodplains. In minor tributaries like Abernethy, Root, Holcomb, and Beaver creeks, the alluvium is predominantly sand and silt on the floodplains with minor pebble and cobble gravel in the channels. Thin deposits of alluvium probably occur in most minor drainages, but alluvium is mapped only where the lidar DEM indicates a significant width (approximately 10 m or more) of flat floodplain. The age of the alluvium in most streams is Holocene, as most of the streams would have been affected by the latest Pleistocene Missoula floods and any alluvial deposits must postdate the floods. Borehole data from the alluvial deposits between the Willamette and Clackamas rivers suggest that cobble gravel extends to a depth of about 15 m.

Qty, Qt, Qto terrace deposits (late Pleistocene-Holocene)—silt and sand (?) deposits capping strath terraces inset into Missoula Flood deposits along Abernethy Creek and the Willamette River near its confluence with the Clackamas River. The terraces occur at three distinct elevations with respect to the modern floodplains of the Willamette River and Abernethy Creek: 10 m (Qty), 15 m (Qt), and 20 m (Qto). No field data indicate the nature or thickness of any deposits on the terraces; the deposits are defined exclusively on the basis of geomorphology interpreted from the lidar DEM. Limited well data suggest that the deposits are silt, sand, and clay. The terraces must be latest Pleistocene to Holocene, as the terraces postdate the Missoula Flood deposits and have been incised as much as 20 m by the modern streams.

Qf flow and fan deposits (late Pleistocene-Holocene)—mixed sand, silt, clay, gravel, and soil deposited by earthflows or debris flows. These deposits are mapped entirely on the basis of subtle topography revealed by the lidar DEM (Figure 3). The deposits generally take one of two forms: 1) fan-shaped deposits at the mouths of small gullies that may be separated from the area where the flow originated by some distance, or 2) lobes on slopes that are more clearly connected to an arcuate hollow upslope where the flow originated. Earth and debris flows typically occur during periods of high rainfall and can be triggered by human activities that concentrate runoff on slopes. These flows can move rapidly down slopes and channels and may be life-threatening. The earthflows and debris flows typically occur on steep slopes underlain by Troutdale Formation or Missoula Flood Deposits. Many debris flows that occurred during the 1996-1997 rain-induced landslide events were reported by Hofmeister (2000) and are indicated on the map, although none could be identified in the lidar DEM.

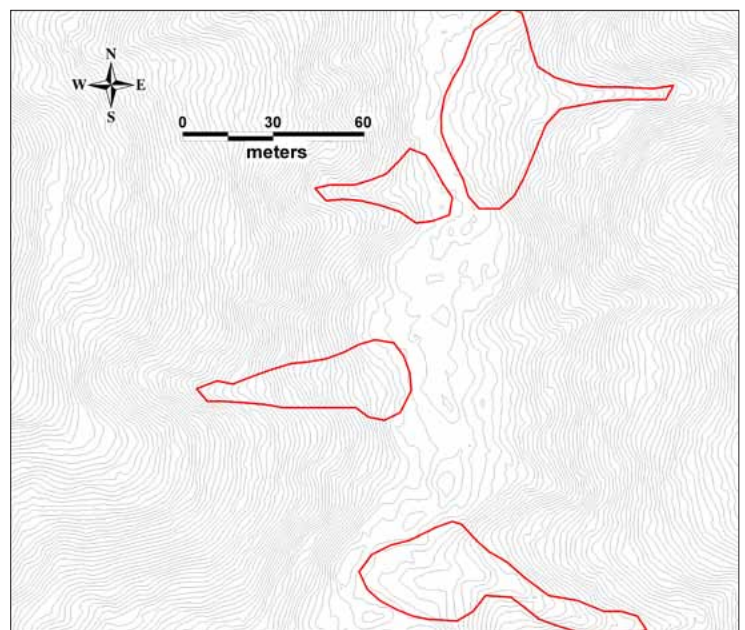


Figure 3. Red lines outline debris flow-earthflow fans visible in 0.6-m contours derived from the lidar digital elevation model (DEM). Fans occur at the mouths of minor gullies emptying into Newell Creek, located in Section 5, T. 3 S., R. 2 E.

Qff Missoula (Bretz) flood deposits (late Pleistocene)—silt, sand, and minor gravel, deposited by floods caused by the repeated failure of the glacial ice dam that impounded glacial Lake Missoula (Bretz and others, 1956; Baker and Nummedal, 1978; Waitt, 1985; Allen and others, 1986). Typically deposited in fining-upward beds; each bed is inferred to represent a single flood event. Exposures are generally poor in the map area, but one spectacular exposure (Figure 4) illustrates several important flood deposit features. In this outcrop the sediment is predominantly fine to medium silty micaceous quartzo-feldspathic sand, deposited in beds 30 to 100 cm thick. The beds are typically capped by zones of brown clay and iron oxide mottling 5 to 30 cm thick that are interpreted to be paleosols. The beds range from massive to laminated and in some instances are ripple cross-bedded. Discontinuous pebble beds 10 to 20 cm thick occur, and sand dikes up to 20 cm wide cut several beds in sequence. In more typical exposures in road cuts and foundation excavations the flood deposits are typically soft brown micaceous quartzo-feldspathic silty fine sand and silt. Rare exotic (granitoids) glacial erratics up to 1 m across are found in the fine-grained facies at elevations up to 115 m.

The flood deposits generally form low terraces in the lower reaches of Parrot, Beaver, and Abernethy creeks and mantle slopes up to elevations of about 60 to 75 m. The deposits are about 10 m thick in the lower reaches of Beaver Creek, 15 m thick in the lower reaches of Parrot Creek, and as much as 24 m thick in the lower reaches of Abernethy Creek.

The age of the flood deposits is estimated to be between 19,000 to 13,000 years B.P. (Mullineaux and others, 1978; Waitt, 1987; Benito and O'Connor, 2003) from tephra and ^{14}C ages from outside the map area.

Qls landslides (Pleistocene–Recent)—chaotically mixed and deformed masses of rock, colluvium, and soil that have moved downslope. Almost 400 landslides were mapped, covering 9% of the quadrangle. Landslide deposits range from about 0.01 hectare up to complexes of slides as large as 88 hectares. The average landslide deposit covers about 3 hectares. Landslides occur almost exclusively where Boring Lava overlies Troutdale Formation along the edge of a canyon and are typically a combination of a block slide and rotational slump. Head scarps are typically steep, up to 20 m high, and commonly have a graben formed at the base (Figure 5). Slide surfaces range from hummocky with numerous scarps and depressions to relatively flat. The top surfaces of the slides are typically littered with large blocks of Boring Lava, in many cases at elevations 15 to 24 m lower than the base of the lava outcrops in the adjacent slope. In several exposures of landslid Troutdale Formation just off the eastern edge of the map, dips up to 35 degrees were observed, along with numerous minor faults. Scattered well data indicate that the slide masses range from 6 to 24 m thick. The majority of large slides on the map were initially identified on the basis of topography observed on aerial photos. The high-resolution DEM based on the lidar data provided striking images of landslide head scarps, internal scarp and graben topography, and lobate toes (Figure 6) and made it possible to map large slides more accurately and to identify numerous smaller slides.

In some cases field observations of chaotic topography, scarps, and displaced lava were made, and in many instances, upright old growth stumps up to 1.2 m in diameter were observed on the surfaces of large landslides, indicating at least centuries of stability. In very few instances indications of recent movement, such as fresh scarps, open ground cracks, or tilted trees, were observed.

The majority of large landslides occur on slopes that would have been largely inundated by Missoula flood waters reaching elevations of approximately 115 m as indicated by erratics. It is possible that many of these slides were initially triggered by saturation of the slopes during flood high stands followed by rapid drawdown as the floods receded.

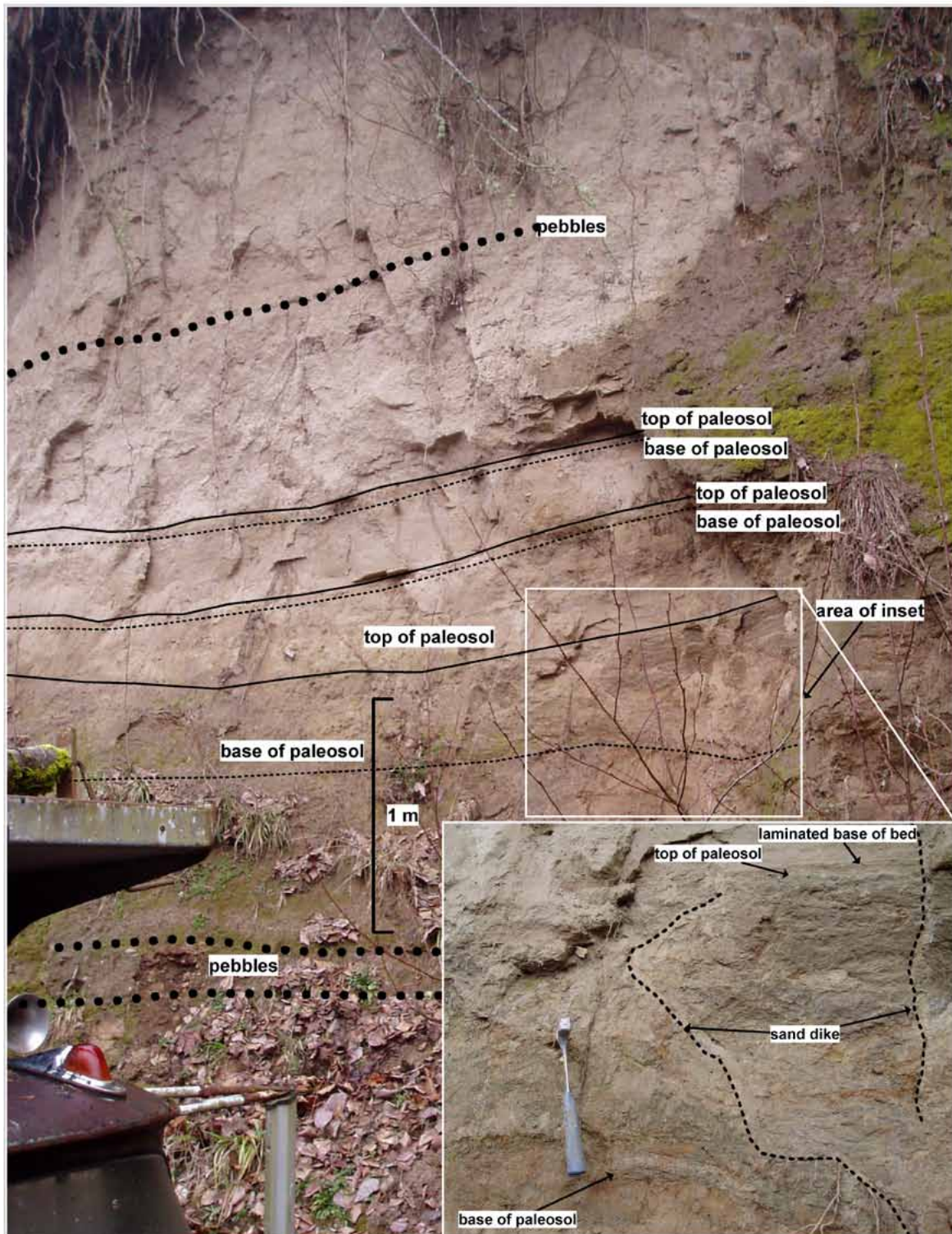


Figure 4. Missoula (Bretz) flood deposits (unit Qff) outcrop. Photo of cut face, approximately 7 m high. Exposure includes several beds up to 1 m thick, with well-developed paleosols, scattered pebble lenses, and sand dikes. Located at station PDX-431.



Figure 5. Landslide graben. Photo (PDX-538) of headwall graben in large landslide complex south of Henrici Road along the east edge of the map. Head scarp in background is approximately 15 m high. Boring Lava blocks from the downhill wall of the graben are visible on left of photo. Hatched lines approximate the graben boundaries, with ticks on downthrown side. Stump indicated in photo is from an upright old-growth Douglas fir tree and is approximately 1.2 m in diameter, indicating several hundred years of stability.

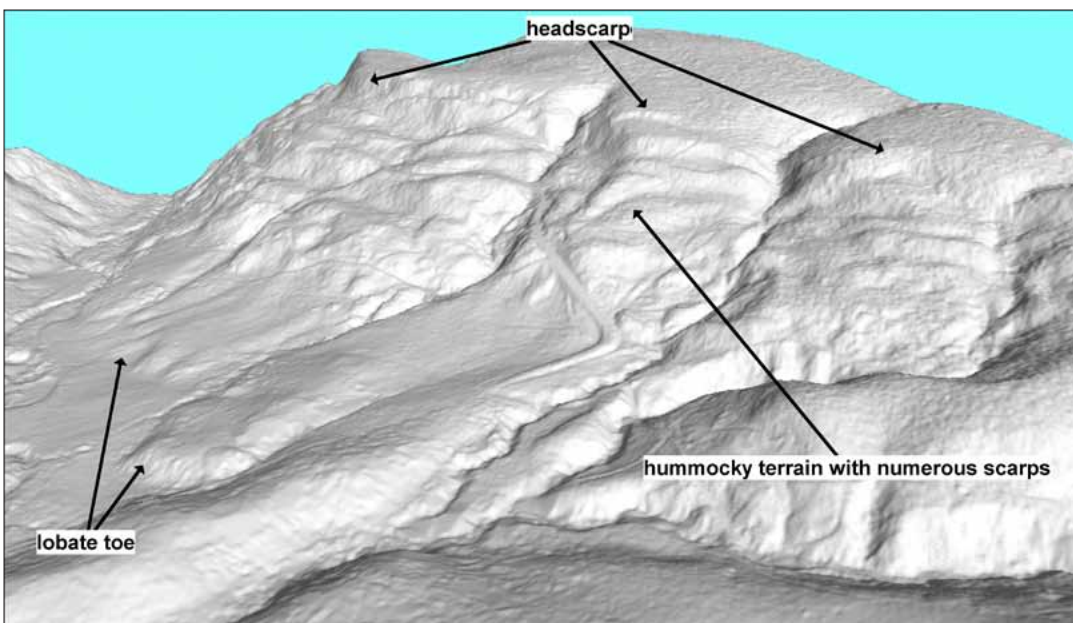


Figure 6. Landslide features visible in lidar digital elevation model (DEM). Perspective view to the southeast of a 44-hectare landslide deposit near the east edge of the map in Section 11, T. 3 S., R. 2 E. Scale varies in this view, which is approximately 1.3 km wide with an elevation range of 100 m. Vertical exaggeration approximately 2.

Boring Volcanic Field Rocks

Numerous small volcanoes and associated basalt flows in the Portland area have been informally known as the Boring Lava, named for exposures near the town of Boring, Oregon (Treasher, 1942). As increased geochemical and geochronological data for these volcanic rocks became available, Fleck and others (2002) proposed that these rocks be considered part of the Boring volcanic field. As used in this study, the Boring volcanic field comprises all of the late Pliocene to Pleistocene mafic volcanoes and lava flows in the greater Portland basin. Within the Oregon City quadrangle, these rocks can be separated out on the basis of lithology, geochemistry, age, and spatial distribution into several units described below.

Qbo basaltic andesite of Outlook (Pleistocene)—flow or flows of fine-grained grey diktytaxitic olivine basaltic andesite (Figure 7). The basaltic andesite of Outlook occurs in the northeast quarter of the map and overlies the Troutdale Formation and Springwater Formation sedimentary rocks and is inferred to overlie the basaltic andesite of Hunsinger. The basaltic andesite of Outlook is not overlain by any younger units in the map area. The unit correlates to the basalt of Outlook of Madin (1994), which was named for exposures near the community of Outlook located north of the northeast corner of the map.

The basaltic andesite of Outlook is rarely exposed but is generally massive, with jointing restricted to crude columns 0.6 to 1.5 m in diameter. Weathered lava is typically grey or purplish and soft, with relict igneous textures preserved.

Petrographically (Figure 8), the basaltic andesite of Outlook is fine grained, moderately pilotaxitic, and diktytaxitic and consists of plagioclase laths up to 0.25 mm long, intergranular clinopyroxene, and interstitial black glass. Slightly to strongly iddingsitized olivine phenocrysts up to 1 mm in diameter are abundant.

Geochemically, the unit is a basaltic andesite (Figure 9) and, compared to other Boring volcanic field units in the map area, has relatively high Na_2O , (average 3.8 %), Ba (average 371 ppm), and Sr (average 737 ppm) and relatively low TiO_2 (average 1.22%), FeO (average 8.15%), and CaO (average 7.35%). In a plot of Sr versus Cr (Figure 10) unit Qbo is easily distinguished from all other units except the basaltic andesite of Hunsinger. It can be distinguished from the basaltic andesite of Hunsinger by its lower MgO (5.6 to 6.0% versus 6.1 to 7.0%). Samples from the vent area near the northeast corner of the map have distinctly higher Sr (Figure 10) than the rest of the unit but are otherwise chemically indistinguishable. Geochemically analyzed samples are plotted on the map, and analytical data are provided in Appendix D.

The contact between the basaltic andesite of Outlook and the underlying Troutdale Formation was observed at only one exposure in a construction site (located at PDX-263) where severely weathered yellow, red, and orange lava with some hard grey fresh blocks overlay yellow, tan, and gray mudstone on a generally planar and smooth contact. Well data suggest that there is considerable relief on the basal contact, and the flows most likely fill canyons cut in the underlying sedimentary rocks.



Figure 7. Hand specimen of basaltic andesite of Outlook (PDX-377). Grid on paper is 3 mm.



Figure 8. Petrography of basaltic andesite of Outlook (PDX-377). Scanned images of petrographic billet (left), slide in plane-polarized light (center), and slide in cross-polarized light (right). Each image is 2.25 cm wide. Brightly colored grains in right-hand image are olivine.

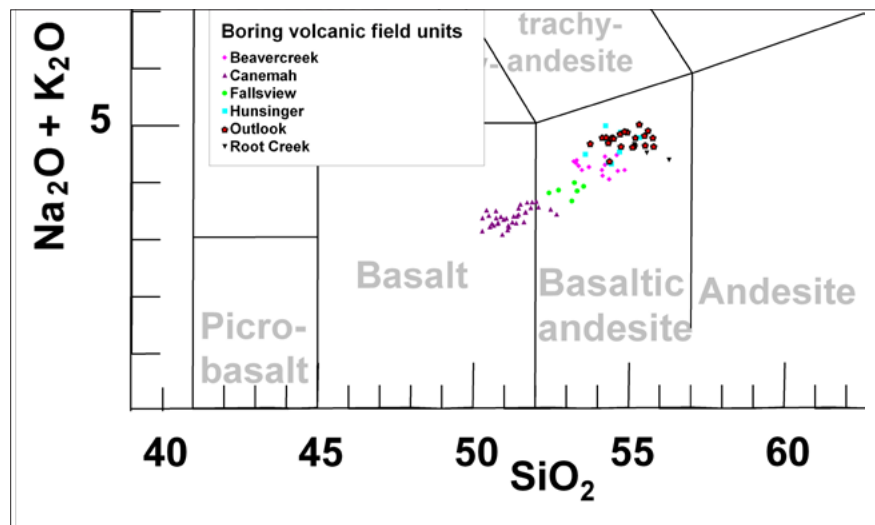


Figure 9. Boring volcanic field lava composition. Boring volcanic field data from this study plotted on the compositional diagram of LeBas and Streckeisen (1989).

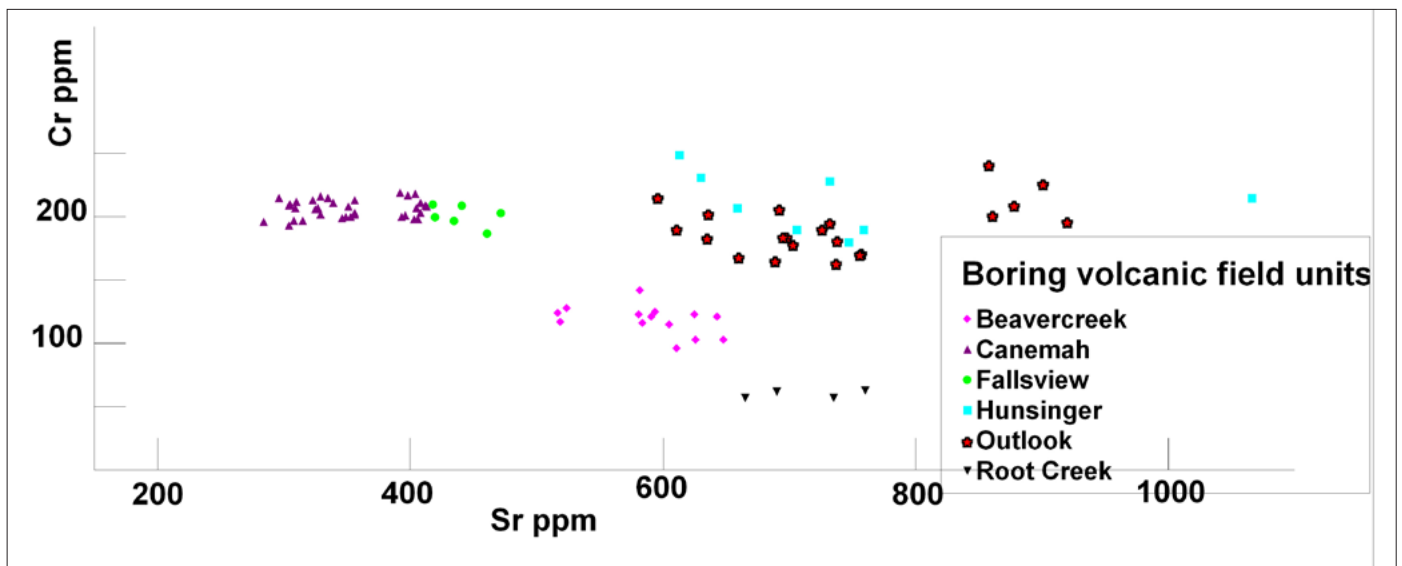
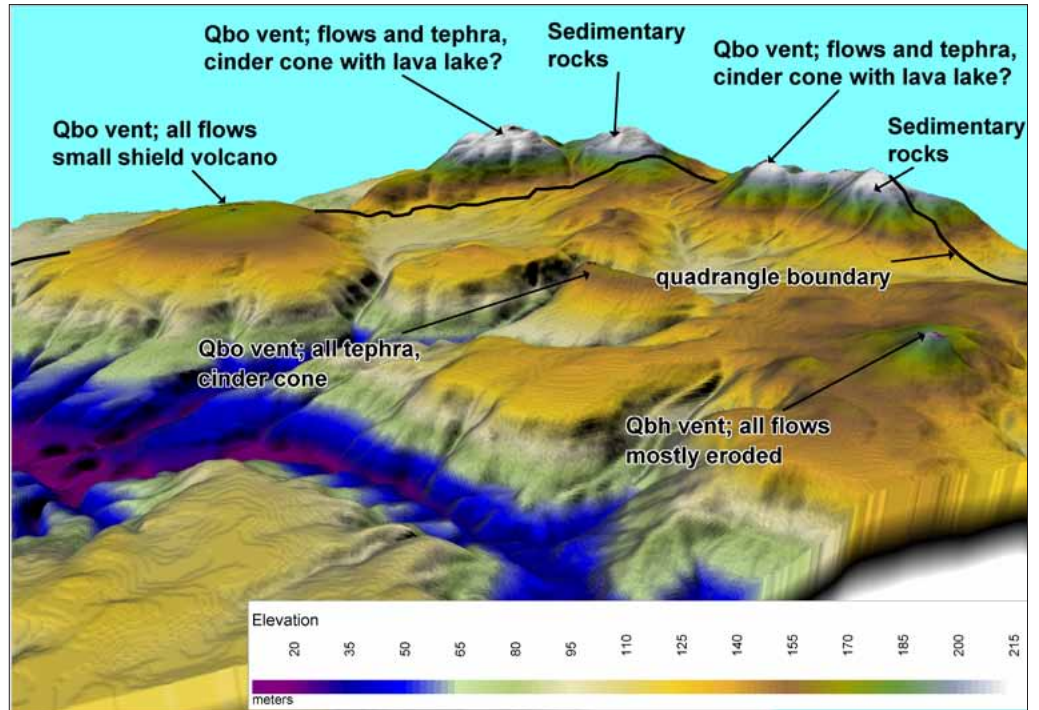


Figure 10. Cr versus Sr plot of Boring volcanic field rocks.

Figure 11. Volcanic vents. Three-dimensional perspective view of the northeast area of the map, looking toward the northeast corner. Five Boring Lava vents are present in or immediately adjacent to the quadrangle. Scale varies in this view, which spans approximately 5 km.



The basaltic andesite of Outlook forms two topographic highs separated by a relatively flat intervening plateau. In the northeast corner of the map area, thin flows of lava emanate from a vent that forms an irregular conical hill (Plate 1 and Figure 11). Along the north-central edge of the map, the unit forms a broad dome-shaped volcano along Holcomb and Hilltop roads; water well logs indicate that it is underlain entirely by flow rocks. The floor of the valley between these two highs probably represents distal flows from the vent in the northeast corner. There is a small vent composed almost entirely of tephra (unit Qvo) just northwest of the intersection of Redland and Bradley roads. A fourth vent of the basaltic andesite of Outlook is located just off the northeastern edge of the map (Figure 11).

Three radiometric ages are available for this unit. Madin (1994) reported a conventional K/Ar date of $3,146 \pm 62$ ka for the basalt of Outlook near Carver, approximately 1.6 km north of the northeast corner of the map. A more recent $^{40}\text{Ar}/^{39}\text{Ar}$ age on the same outcrop at Carver yielded an age of $1,220 \pm 50$ ka (Russell Evarts, personal communication, 2005). An $^{40}\text{Ar}/^{39}\text{Ar}$ age from this study (PDX-501, Appendix F) gave a plateau age of $1,280 \pm 40$ ka. All measured outcrops had reversed remnant magnetic polarity.

The basaltic andesite of Outlook is typically 15 to 60 m thick north of Redland Road and east of Bradley Road but is 60 to 80 m thick in the small shield volcano along Holcomb Road. The approximate volume of the lava within the map area is estimated to be about 0.2 km^3 .

Qvo Outlook tephra (Pleistocene)—ash, scoria, bombs, and breccia of basaltic andesite of Outlook composition deposited on and around vents. The tephra is exposed around the vent in the far northeast corner of the map (Figure 11) and in a small cinder cone northwest of the intersection of Redland and Bradley roads. In most exposures the tephra is severely weathered to clay and is brightly colored in shades of tan, pink, red, orange, yellow, white, and black. At the small cinder cone this unit includes bombs up to 30 cm long. At the vent in the northeast corner, the tephra is interbedded with thin vesicular lava flows, sandstone, and mudstone and includes cobbles from the underlying Springwater Formation.

Bomb or breccia fragments were geochemically analyzed from both vent deposits and correlate geochemically with the basaltic andesite of Outlook. From correlation with the dated flows of the basaltic andesite of Outlook, the vent deposits are likely to be Pleistocene in age.

The tephra is about 45 m thick in the northeast corner and about 70 m thick at the small cinder cone.

Qbh basaltic andesite of Hunsinger (Pleistocene)—flow or flows of grey fine-grained, diktytaxitic olivine basaltic andesite (Figure 12). This unit covers much of the northeast corner of the quadrangle, exclusively northeast of Abernethy Creek, and is named for the benchmark (Section 2, R. 3 S., T. 2 E.) on the small hill that coincides with the inferred vent for the flows. The unit overlies the Troutdale Formation and the Springwater Formation and is overlain locally by the basaltic andesite of Outlook. Although the basaltic andesite of Hunsinger and the older basalt of Canemah occur at the same elevation on both sides of Abernethy Creek, it was not possible to find evidence of overlap. The basaltic andesite of Hunsinger is typically massive, with widely spaced planar joints (Figure 13). Weathered surfaces are typically littered with subangular blocks up to 1 m across. Petrographically (Figure 14), the lava is fine-grained, weakly pilotaxitic, and consists of plagioclase laths up to 0.5 mm long, with intersertal black glass. Abundant slightly iddingsitized olivine up to 1.5 mm in diameter is commonly rimmed with fine grains of magnetite. Rare euhedral plagioclase phenocrysts to 1.5 mm occur and distinguish the basaltic andesite of Hunsinger from the basaltic andesite of Outlook. The rock is weakly pilotaxitic and weakly to strongly diktytaxitic.

Geochemically, the basaltic andesite of Hunsinger is a basaltic andesite (Figure 9) and, compared to other Boring volcanic field units in the map area, has relatively high Na_2O , (average 3.8 %) and Sr (average 739 ppm) and relatively low TiO_2 (average 1.14%), FeO (average 7.65%), and CaO (average 7.9%). In a plot of Sr versus Cr (Figure 11) it is easily distinguished from all other units except the basaltic andesite of Outlook. It can be distinguished from the basaltic andesite of Outlook by its higher MgO (6.1 to 7.0% versus 5.6 to 6.0%). Geochemically analyzed samples are plotted on the map, and analytical data are provided in Appendix D.

The contact between this unit and the underlying Troutdale Formation was not observed, but the map pattern suggests that the flows locally fill steep-sided canyons.

The basaltic andesite of Hunsinger appears to have erupted from a vent located at the small hill located about 600 m ESE of the intersection of Beckman and Ferguson roads. The hill is inferred to be a vent because it is underlain by massive lava and is currently the highest point occupied by the unit.

A sample of the basaltic andesite of Hunsinger from Maple Lane yielded an $^{40}\text{Ar}/^{39}\text{Ar}$ age of $1,217 \pm 89$ ka, and a sample from Potter Creek had an $^{40}\text{Ar}/^{39}\text{Ar}$ age of $1,190 \pm 10$ ka (Russell Evarts, personal communication, 2005). All measured outcrops were magnetically reversed.

The basaltic andesite of Hunsinger is typically 45–75 m thick, and the estimated volume of lava remaining in the area is 0.24 km^3 .

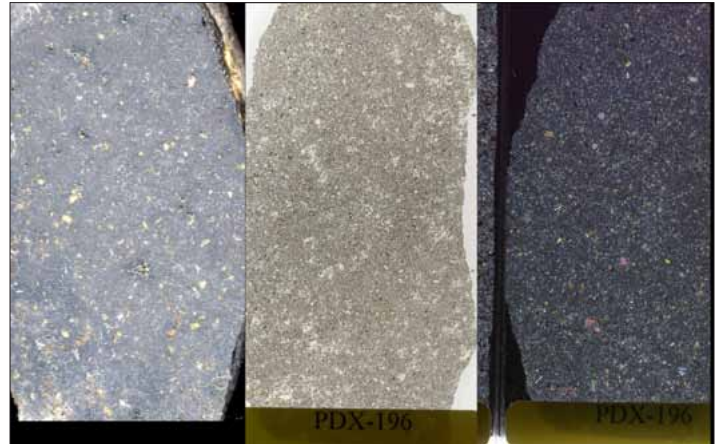


Figure 12. Hand specimen of basaltic andesite of Hunsinger (PDX-196). Grid on paper is 3 mm.



Figure 13. Basaltic andesite of Hunsinger. Outcrop in quarry (PDX-196). Note massive character, lack of joints.

Figure 14. Petrography, basaltic andesite of Hunsinger (PDX196). Scanned images of petrographic billet (left), slide in plane-polarized light (center), and slide in cross-polarized light (right). Images are 4.25 by 2.25 cm. Yellow-green grains in left-hand image and brightly colored grains in right-hand image are olivine.



Tbc basalt of Canemah (Pliocene)—flow or flows of dark grey medium-grained, diktytaxitic olivine basalt (Figure 15). The basalt flows underlie much of the center of the quadrangle and extend nearly continuously from the southeast corner of the map to the edge of the Willamette River canyon in the northwest corner of the map. The basalt of Canemah overlies the Troutdale Formation throughout most of its mapped range and is overlain only by Missoula Flood deposits in Oregon City. Stratigraphic relations with the other lavas of the Boring volcanic field could not be conclusively established, but the basalt of Canemah is inferred to overlie the basalt of Beaver Creek and the basalt of Fallsview on the basis of data from water well logs. The unit is informally named in this study for exposures near the small community of Canemah in Section 1, T. 3 S., R. 1 E.

The basalt of Canemah is typically massive, with jointing restricted to well-developed to crude columns 0.6 to 1.5 m across (Figure 16). Weathering along the joint faces leads to the development of spheroidal weathering (Figure 17) that typically extends to depths of 3 to 6 m. In many excavations, all that is left are scattered large rounded corestones in a matrix of red clay. Intact weathered basalt is typically soft and grey, white or pink, with abundant red clay coatings on joint faces. Recognizable relict igneous texture is preserved.

Petrographically (Figure 18), the basalt of Canemah is fine to medium grained and consists of plagioclase laths up to 1 mm long, intergranular clinopyroxene, and small amounts of black glass. Slightly to strongly iddingsitized olivine up to 1 mm in diameter is abundant.

Geochemically, the basalt of Canemah (Figures 10 and 11) is chemically distinct, with higher FeO (average 10.94%), MgO (average 7.14%), and CaO (average 8.93%) and lower K₂O (average 0.42 %), P₂O₅ (average 0.16%), Sr (average 355 ppm), and Ba (average 132 ppm) than any of the other Boring volcanic field units in the map area, which are all basaltic andesites. Geochemically analyzed samples are plotted on the map, and analytical data are provided in Appendix D.

The contact between the basalt of Canemah and the underlying Troutdale Formation is rarely exposed, but at two excellent outcrops (Figure 19) the contact was sharp, was conformable with the bedding in the underlying sedimentary rocks, and did not have any basal breccia or baked zone. Water well data were used to prepare a structure contour map on the base of the basalt of Canemah (Figure 20). The base generally descends in elevation from about 150 m in the southeast corner to about 100 m near Canemah along the southeast slope of the Willamette River canyon. This gentle sloping surface has some relief, with buried canyons and ridges that are up to 15 m deep as indicated by the structure contour map. In the slopes above Canemah, excellent exposures of the basalt in road cuts (Figure 21) are different in appearance from most other exposures. At this site, numerous thin lobes of basalt are separated by breccia zones, and partially collapsed lava tubes are present. These features suggest that the lava may have been flowing over a steep slope descending into the canyon of the Willamette River. The absence of Boring Lava north and west of the Willamette River in the map area suggests that the river acted as a barrier to the northwestward progression of the flows.

The upper surface of the basalt of Canemah forms a gently undulating plateau that slopes gradually in elevation from about 180 m in the southeast to about 135 m at Oregon City to the northwest. The basalt is deeply incised by



Figure 15. Hand specimen of basalt of Canemah (PDX-130). Grid on paper is 3 mm.



Figure 16. Jointing in basalt of Canemah. Columns in left photo (PDX-130) are 0.6 to 1.2 m in diameter; columns in right photo are 1.5 m in diameter (PDX-535).

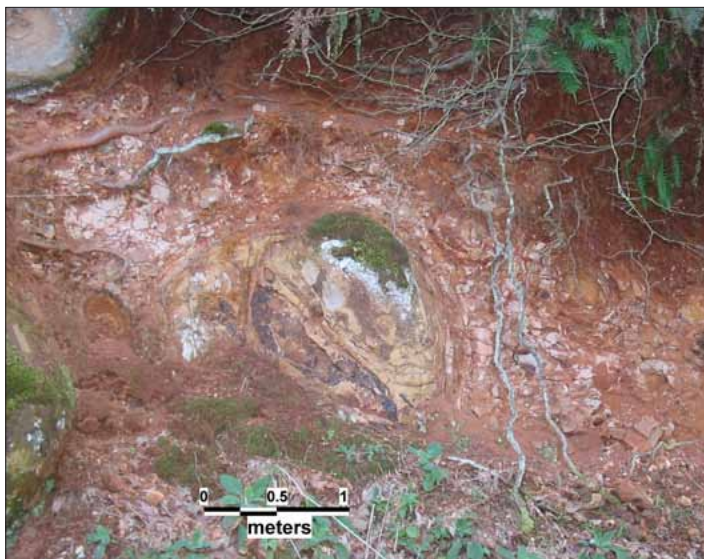


Figure 17. Weathering, basalt of Canemah. Spheroidal weathering in basalt of Canemah results in large rounded corestones embedded in grey or red soft basalt or clay. Located at PDX-525.

Figure 18. Petrography, basalt of Canemah (PDX-130). Scanned images of petrographic billet (left), slide in plane-polarized light (center), and slide in cross-polarized light (right). Images are 4.25 by 2.25 cm. Brightly colored grains in right-hand image are olivine.

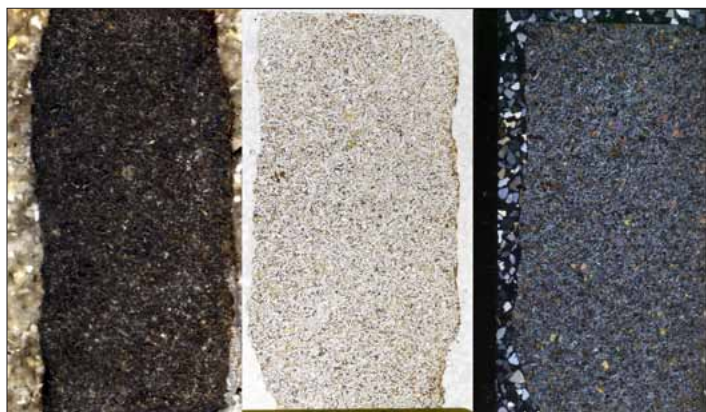


Figure 19. Basal contact, basalt of Canemah. Sharp, conformable contact between basalt of Canemah (above) and flat-lying thin-bedded Troutdale Formation sandstone (below). No basal flow breccia or baked zone exists in the sedimentary rock. Arrows mark contact. Located at PDX-536.

Figure 20. Basalt contact surface data. Contours give the elevation of the base of basalt of Canemah in meters, blue dots are wells that define base, and grey tint is extent of unit. Pink tint shows extent of outcrops of Columbia River Basalt Group (CRBG), and red diamonds are locations of wells that define the elevation of the top of CRBG, labeled with the top elevation in meters. Black outline is quadrangle boundary, and heavy black lines are faults.

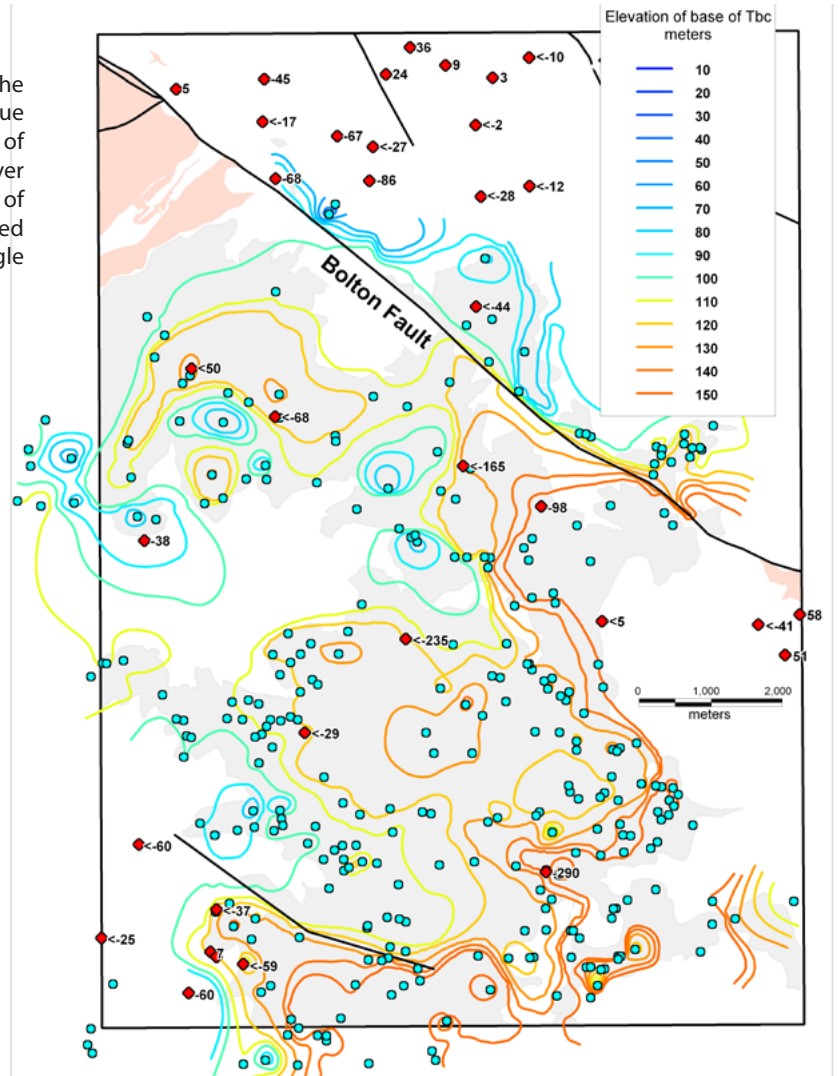


Figure 21. Lava tube, basalt of Canemah. Partially collapsed lava tube approximately 2 m wide in the basalt of Canemah, above Canemah. Located at PDX-127.

the major streams in the map area, with many canyons cut through as much as 24 to 30 m of lava and another 60 m of Troutdale Formation.

The basalt of Canemah was probably erupted in part from inferred vents near the southeast corner of the map. One inferred vent caps the hill in Section 35, T. 3 S., R. 2 E., and the other is just off the map to the southeast, near the community of Massinger's Corner. The vents are inferred where flows of the basalt of Canemah are interbedded with thick deposits of tephra, as indicated by water well logs. The lava was probably fairly fluid, as it advanced at least 15 km from the vents in the southeast corner to reach the Willamette River in the northwest corner.

There are several radiometric ages available for the basalt of Canemah. Conrey and others (1996) reported a conventional K/Ar date of $2,440 \pm 180$ ka from flows at the Water Board Park in Oregon City (geochemical sample code BJ, field station PDX-130). A more recent date from the adjacent Colton quadrangle (southeast) gives an $^{40}\text{Ar}/^{39}\text{Ar}$ age of $2,530 \pm 40$ ka (Russell Evarts, personal communication, 2005). All measured outcrops of the basalt of Canemah had reversed remnant magnetic polarity.

The basalt of Canemah is typically 15 to 40 m thick (Figure 22) and is generally thickest to the southeast nearer the vents. The volume of the flow can be estimated by subtracting a gridded basalt contact surface derived from the contours in Figure 20 from a DEM of the ground surface. The result indicates a minimum volume within the mapped area of 1.4 km^3 , based on just the mapped extent of the unit. Erosion has probably removed a similar amount from the original volume of this unit within the quadrangle.

The weathered top of the basalt of Canemah is locally overlain by massive red-brown to brown sandy silty clay. The material is apparently sedimentary in origin, comprising a matrix of red-brown to brown clay with variable amounts of rounded heterogeneous lithic sand, silt, fine lithic and feldspathic sand, and rare angular quartz sand. The material is clearly distinct from the severely weathered basalt it overlies; in the rare instances that the contact is observed it is sharp. The unit has a patchy distribution and, from water well logs, is probably never more than 1-3 m thick; therefore it is not mapped. The origin of the deposits may include airfall tephra from later Boring eruptions, windblown sediment, and an alluvial component from the earliest drainages that were established on the surface of the basalt of Canemah.

Tvc Canemah tephra (Pliocene)—ash to bomb size tephra with minor basalt flows inferred from water well logs. The tephra caps the hill in Section 35, T. 3 S., R. 2 E. and forms an irregular cone around the inferred basalt of Canemah vent located just off the map at Massinger's Corner. No outcrops of the tephra were observed, but water well logs in the area suggest that the tephra is mixed with thin flows of lava. Well log descriptions indicate that much of the tephra is largely weathered to clay. Nearby flows were sampled for geochemical analysis and were correlated chemically with the basalt of Canemah.

Well logs indicate that the deposit is approximately 35 m thick at the vent in Section 35, T. 3 S., R. 2 E., and at least 54 m thick near Massinger's Corner.

Tbr basaltic andesite of Root Creek (Pliocene)—flow or flows of fine-grained grey basaltic andesite (Figure 23). The basaltic andesite occurs only in the southeast corner of the map, along Root Creek, after which the basalt is named. The unit overlies the Troutdale Formation and Root Creek tephra. The basaltic andesite of Root Creek is not overlain by any younger units in the map area.

The unit is rarely exposed but is typically strongly platy (Figure 24).

Petrographically (Figure 25), the basaltic andesite of Root Creek is fine-grained, strongly pilotaxitic, and has no vesicles. The rock consists of plagioclase laths up to 0.4 mm long, with intergranular to subophitic clinopyroxene up to 0.1 mm, and interstitial opaques or black glass. Olivine is absent, making this unit unique among Boring volcanic field flows in the map area.

Geochemically, the basaltic andesite of Root Creek is a basaltic andesite (Figure 9) and, compared to other Boring volcanic field units on the map, has the highest TiO_2 (average 1.4%), Al_2O_3 (average 18.11%), and K_2O (average 0.98%) and lowest MgO (average 3.95%), CaO (average 7.24%), and Cr (60 ppm). The low MgO and Cr reflect the absence of olivine in the rock. The unit is also clearly distinct from the other Boring volcanic field units on the plot of Sr versus Cr (Figure 10). Geochemically analyzed samples are plotted on the map, and analytical data are pro-

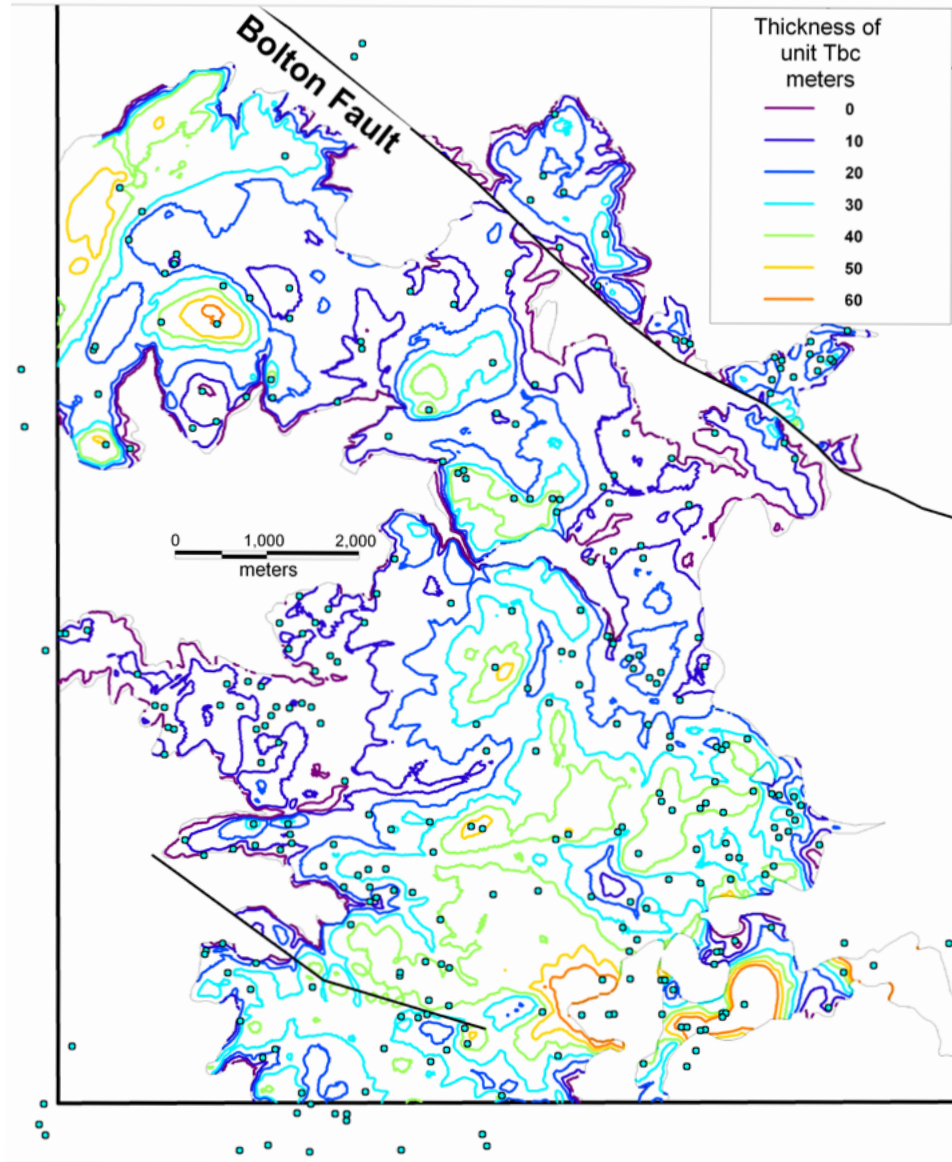


Figure 22. Isopach map for the basalt of Canemah. Faint grey line outlines extent of basalt of Canemah; heavy black lines are faults; black box is quadrangle boundary.



Figure 23. Hand specimen, basaltic andesite of Root Creek (PDX-56). Grid on paper is 3 mm.



Figure 24. Basaltic andesite of Root Creek. Exposed in road cut (PDX-56). Note platy jointing; hammer for scale.

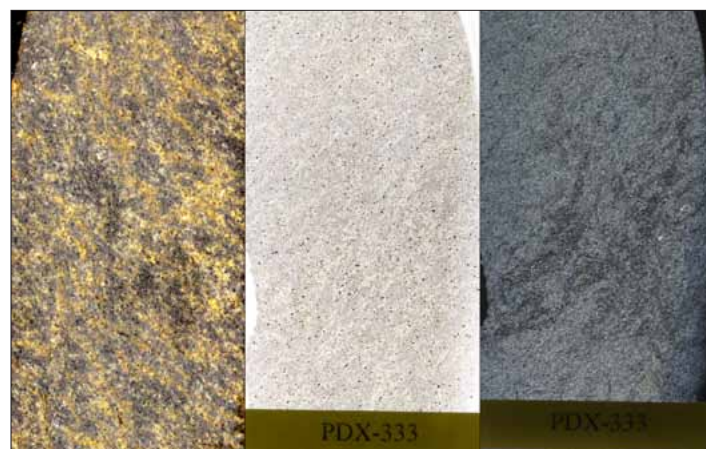


Figure 25. Petrography, basaltic andesite of Root Creek (PDX-333). Scanned images of petrographic billet (left), slide in plane-polarized light (center), and slide in cross-polarized light (right). Images are 4.25 by 2.25 cm. Dark grains in center and right-hand images are magnetite.

vided in Appendix D.

The contact between the basaltic andesite of Root Creek and the underlying Troutdale Formation was not observed, but outcrop patterns and water well data suggest that the flows filled a steep-sided north-trending canyon approximately 100 m deep.

The basaltic andesite of Root Creek was erupted from a vent just off the map to the east, about 1 km from PDX-56. The vent is a conical hill composed of olivine-free scoria, with chemistry (Russell Evarts, personal communication, 2005) matching that of the Root Creek flows.

Russell Evarts (personal communication, 2005) reported an $^{40}\text{Ar}/^{39}\text{Ar}$ total fusion age of $2,470 \pm 20$ ka. The unit has normal remnant magnetism based on fluxgate magnetometer data from a single site. Russell Evarts (personal communication, 2005) reported that the unit has reversed remnant magnetism based on more sophisticated measurements.

Limited well data suggest that the basaltic andesite of Root Creek is 90 m thick. Although the extent of the unit on the Redland quadrangle to the east is unknown, it is likely that the volume of the unit in the map area is quite small.

Tvr Root Creek tephra (Pliocene)—ash, scoria, bombs, and breccia of basaltic andesite of Root Creek composition. The tephra is exposed only along the eastern edge of the map, in road cuts where Carus Road crosses Root Creek. The tephra is severely weathered and consists of red brown ash matrix with yellow, soft, weathered scoria and black bombs up to 80 cm across. The bombs typically have a scoriaceous crust, and some larger ones have relatively fresh cores. The tephra underlies flows of the basaltic andesite of Root Creek and overlies mudstones and sandstones of the Troutdale Formation.

Bomb fragments were geochemically analyzed from the tephra deposits and correlate geochemically with the basaltic andesite of Root Creek. The tephra are likely to be Pliocene, from correlation with the flows of the basaltic andesite of Root Creek.

The thickness of the tephra is poorly constrained but is estimated to be 3 to 9 m.

Tbf basaltic andesite of Fallsview (Pliocene)—flow or flows of grey to black, fine to medium-grained, diktytaxitic olivine basaltic andesite (Figure 26). The flows occur only in the southeast and southwest parts of the map area, where they are interbedded with tephra of Fallsview, but are widespread to the south on the Mollala quadrangle, where they are named for outcrops near the community of Fallsview (Russell Evarts, personal communication, 2005). The unit overlies the Fallsview tephra and is inferred to be overlain by the basalt of Canemah. The basaltic andesite of Fallsview typically has widely spaced joints, and the ground surface on the unit is typically littered with subangular boulders.

Petrographically (Figure 27), the lava is medium-grained and consists of plagioclase laths up to 1.5 mm long, intergranular pyroxene, interstitial masses of black opaques, and abundant moderately to strongly iddingsitized olivine up to 1.5 mm in diameter. The rock is moderately pilotaxitic and diktytaxitic.

Geochemically, the basaltic andesite of Fallsview is a basaltic andesite (Figure 9) but is intermediate in composition between the basalt of Canemah and the other basaltic andesite units (Figures 9 and 10). Compared to the other basaltic andesite units, it has higher FeO (average 10.15%) and lower K_2O (average 0.59%), P_2O_5 (average 0.22%), Ba (average 201 ppm), and Sr (average 441 ppm). Compared to the basalt of Canemah, it has lower FeO and MgO (average 5.64%) and higher K_2O . Geochemically analyzed samples are plotted on the map, and analytical data are provided in Appendix D.

The contact between this unit and the surrounding tephra is well exposed in a road cut in Section 2, T. 4 S., R. 2 E. Along this cut, an upper flow conformably overlies bedded tephra, which has an irregular contact with the underlying lava flow. The lower lava flow conformably overlies crudely bedded tephra.

Several vents for the basalt of Fallsview occur in and adjacent to the southeast corner of the map (Plate 1). Two vents occur on the map in the west half of Section 2, T. 4 S., R. 2 E. One is a small conical hill underlain by the highest local flows of the unit; the other is a roughly circular depression 180 m across that is inferred to be an eroded crater. A third vent occurs just south of the map along Newkirchner Road (Section 3, T. 4 S., R. 2 E.) and is spec-



Figure 26. Hand specimen of basalt of Fallsview. Grid on paper is 3 mm (PDX-468).



Figure 27. Petrography, basalt of Fallsview (PDX-172). Scanned images of petrographic billet (left), slide in plane-polarized light (center), and slide in cross-polarized light (right). Images are 4.25 by 2.25 cm. Red-brown grains in center and right-hand images are weathered olivine.



Figure 28. Basalt of Fallsview vent. Central dike cuts tephra deposits, merges with thin highly vesicular flow that caps the tephra, located at PDX-172. Dike is approximately 6 m wide.

tacularly exposed in a cut 75 m long (Figure 28). The majority of the cut consists of tephra, which is cut by a central feeder dike of lava about 6 m wide and is capped by a thin, highly vesicular lava flow.

The basalt of Fallsview has been radiometrically dated on the adjacent quadrangle to the south. The sample there yielded an $^{40}\text{Ar}/^{39}\text{Ar}$ age of $2,540 \pm 80$ ka and has reversed remnant magnetism (Russell Evarts, personal communication, 2005).

The thickness of the basalt of Fallsview is variable, ranging from distal flows 3 to 12 m thick to flows 81 m thick near the vents. The volume of lava remaining in the area is difficult to estimate, given the complex interbedding with tephra, but is probably on the order of 0.08 km^3 . There is substantial additional volume on the adjacent Molala quadrangle.

Tvf Fallsview tephra (Pliocene)—ash, scoria, bombs, and breccia interbedded with the basaltic andesite of Fallsview. The tephra is exposed in several cuts near the southeast corner of the map and is always interbedded with or capped by the basaltic andesite of Fallsview. The tephra is severely weathered and consists of red brown ash matrix with white and yellow, soft, weathered scoria and black bombs up to 40 cm across. The bombs typically have scoriaceous crusts, and some larger ones have relatively fresh cores. In one exposure, the tephra are horizontally bedded, with layers ranging from 0.6 to 60 cm (Figure 29).

The tephra overlies mudstone and sandstone of the Troutdale Formation.

No clasts from the deposit were geochemically analyzed. The deposits are correlated to the basaltic andesite of Fallsview on the basis of their interbedded relationship. The tephra is therefore Pliocene on the basis of the radiometric age for the basaltic andesite flows.

The thickness of the tephra is poorly constrained, but water well logs suggest that it is as much as 36 m thick near the vents.

Tbb basaltic andesite of Beaver Creek (Pliocene)—flow or flows of grey fine-grained, weakly diktytaxitic olivine basaltic andesite (Figure 30). The flows cover a few square kilometers in the east-central portion of the map and underlie the community of Beaver Creek, after which the unit is named. The unit overlies the Troutdale Formation and is inferred to be overlain by the basalt of Canemah. The basaltic andesite of Beaver Creek typically has strong platy jointing. In some exposures, weathering proceeds along the platy joints, converting the rock into a soft, white, grey, or tan mass of clay that superficially resembles a bedded sedimentary rock (Figure 31), although relict igneous textures are preserved.

Petrographically (Figure 32), the lava is fine grained and consists of plagioclase laths up to 0.5 mm long, intergranular pyroxene, interstitial masses of black opaques, and abundant strongly iddingsitized olivine up to 1.5 mm in diameter. The rock is strongly pilotaxitic and weakly diktytaxitic.

Geochemically, the basaltic andesite of Beaver Creek is a basaltic andesite (Figure 9) and is clearly distinct from all of the other Boring volcanic field units on the plot of Sr versus Cr (Figure 10). Compared to the other basaltic andesite units the basaltic andesite of Beaver Creek has substantially higher FeO (average 9.26%) and lower K_2O (average 0.82%), Sr (average 590 ppm), Cr (average 118 ppm), and Ba (average 248 ppm). Geochemically analyzed samples are plotted on the map, and analytical data are provided in Appendix D.

The contact between the unit and the underlying Troutdale Formation is never observed, but contact relations and water well data suggest that the flows filled a north-trending steep sided canyon (Plate 1, cross section D-D').

The vent for the basaltic andesite of Beaver Creek has not been located and may be on the Redland quadrangle to the east, where there are numerous conical hills.

The basaltic andesite of Beaver Creek was radiometrically dated (sample PDX-342) for this study (Appendix F), and yielded an $^{40}\text{Ar}/^{39}\text{Ar}$ plateau age of $2,660 \pm 50$ ka. All measured outcrops were magnetically reversed.

The basaltic andesite of Beaver Creek is typically 60 to 70 m thick. The estimated volume of lava remaining in the area is 0.28 km^3 .

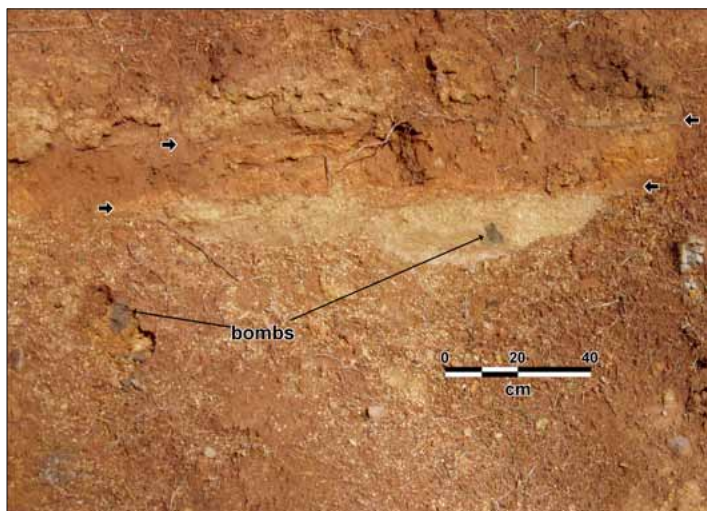


Figure 29. Fallsview tephra. Short arrows indicate bedding in tephra located at PDX-466.



Figure 30. Hand specimen of basaltic andesite of Beaver Creek (PDX-181). Grid on paper is 3 mm.



Figure 31. Basaltic andesite of Beaver Creek. Exposed in road cut (PDX-181). Note platy jointing and severe weathering; hammer for scale.

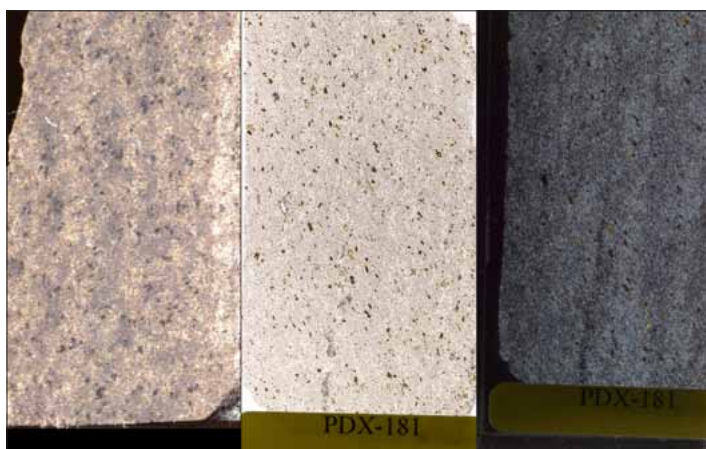


Figure 32. Petrography, basaltic andesite of Beaver Creek (PDX-181). Scanned images of petrographic billet (left), slide in plane-polarized light (center), and slide in cross-polarized light (right). Images are 4.25 by 2.25 cm. Red-brown grains in center and right-hand images are weathered olivine.

Miocene-Pleistocene Fluvial Sedimentary Rocks

Qg conglomerate (Pleistocene?)—pebble to cobble conglomerate exposed in the walls of a small stream canyon in the extreme northwest corner of the map area. The conglomerate consists largely of well-rounded pebbles and cobbles of basalt, andesite, and dacite with a coarse sand matrix composed largely of volcanic lithic fragments and feldspar.

The conglomerate overlies a severely weathered flow top of the basalt of Sand Hollow and is in turn overlain by unconsolidated silt and sand of the Missoula Flood deposits.

The conglomerate was probably deposited by the ancestral Willamette River. The unit is approximately 5 m thick.

QTs Springwater Formation (Pliocene to Pleistocene)—sandstone and conglomerate deposited by the ancestral Clackamas River. The Springwater rocks occur in a band across the northeast corner of the map area where they overlie the Troutdale Formation and are overlain by the basaltic andesites of Hunsinger and Outlook. The unit correlates to the Springwater Formation of Madin (1994) and, in part, to the Springwater Formation of Trimble (1963).

In the map area the Springwater Formation consists largely of pebble, cobble, and boulder conglomerate (Figure 33), which typically has a lithic-feldspathic sand matrix and clasts of basalt, andesite, and dacite probably derived from the Cascade Range. The clasts are typically well rounded and are commonly severely weathered (Figure 33), often to the point where they easily crumble. The conglomerate also includes rare metamorphic quartzite pebbles and cobbles. These highly resistant clasts locally form a lag on the surface as the volcanic clasts weather away. The Springwater Formation commonly consists of white, tan, grey, and brown mudstone and poorly sorted feldspathic-volcanic lithic sandstone; rarely, the unit consists of white or tan mica-bearing sandstone or mudstone. Well records indicate that at least half the thickness of the unit is typically mudstone and sandstone. Contact relations were not observed with either the underlying Troutdale Formation or overlying lavas.

The Springwater Formation conglomerates are fluvial gravels composed predominantly of clasts derived from the Cascade Range and deposited by an ancestral Clackamas River. They include some quartzite gravel and mica-ceous sand reworked from older Troutdale Formation gravels that were deposited by the ancestral Columbia River.

The Springwater Formation is Pliocene to Pleistocene in age. In the Estacada quadrangle approximately 16 km to the east, Springwater Formation overlies a Boring Lava dated at 2.7 Ma (Madin, 2004). In the map area the Springwater Formation is overlain by the basaltic andesites of Outlook and Hunsinger, both of which have been radiometrically dated at about 1.2 Ma.

The Springwater Formation is typically 30 to 45 m thick.

Tt Troutdale Formation (Miocene to Pliocene)—mudstone, claystone, sandstone, and minor conglomerate and tuff. Troutdale Formation rocks underlie most of the quadrangle, with the exception of the northwest corner of the map where they have been largely eroded away. The Troutdale Formation overlies the Columbia River Basalt, and is overlain in places by virtually all of the other units in the map area. The Troutdale Formation correlates with the Troutdale Formation of Trimble (1963) and with the Troutdale Formation of Lite (1992) and Madin (1994, 2004) on the adjacent quadrangles to the north and east. Madin (1994) divided the Troutdale into sandstone (Tts), mudstone (Ttm), and conglomerate (Ttg) units, and the various lithologies probably represent facies of the same large-scale fluvial deposition system. On the Oregon City quadrangle these lithologies are complexly interbedded; it was not possible to map them separately. Figure 34 shows graphic logs for four deep water wells to illustrate the downhole and crosshole variability. Although some variability is due to the fact that a different driller logged each hole, sandstone and gravel are the primary aquifers, so the lack of these units in CLAC 56352 is probably a real geologic variation.

Claystone and mudstone are typically massive, rarely laminated, and white, tan, brown, and grey. Diatoms (*Melosira* sp.), irregular rounded tuffaceous glass blebs, and mica are also common constituents. The rocks are generally weak to moderately strong and support relatively gentle slopes that are very prone to landsliding where overlain by Boring volcanic field flows. Figure 35 shows examples of hand specimens of massive and laminated mudstone, and Figures 36 and 37 show thin sections of the same rocks. PDX-83 is massive and contains 30 to 40% diatom tests. PDX-86A is finely laminated and contains rare diatom tests and abundant irregular rounded blebs of glass. Fig-



Figure 33. Springwater Formation Conglomerate. Located at PDX-264. Note severe weathering resulting in many clasts being cut through during excavation.

metamorphic quartzite-clast conglomerate was observed south of Beckman Road just east of the basaltic andesite of Hunsinger vent. This conglomerate consists almost exclusively of smooth-surfaced, well-rounded red, pink and yellow-tan metamorphic quartzite clasts, with micaceous quartzo-feldspathic sand matrix. Lags of similar pebbles and cobbles are common around the Hunsinger vent.

The age of the Troutdale Formation is poorly constrained in the map area. It overlies the middle Miocene Columbia River Basalt Group, and is overlain by the Pliocene-Pleistocene Boring volcanic field and Springwater Formation. Since these younger units all appear to fill channels cut in the Troutdale Formation, it is likely that deposition of the Troutdale had ceased by the late Pliocene when the eruption of the Boring volcanic field began.

The thickness of the Troutdale Formation varies across the map area, reflecting considerable relief on the top of the underlying Columbia River basalt. The thickest section of Troutdale Formation penetrated by a water well is 345 m in well CLAC 56352 (Figure 34), which did not reach the bottom of the Formation.

In the map area, the Troutdale Formation contains sediments derived from the Columbia River (micaceous

ures 38 and 39 illustrate outcrops of the massive and laminated mudstones. Claystone and mudstone are by far the dominant lithology reported in water well logs that penetrate the Troutdale Formation.

Sandstone ranges from clean, well-sorted micaceous, quartzo-feldspathic sandstone to poorly sorted, poorly rounded feldspar and volcanic lithic sandstone with little or no mica. Hand specimens of both types are shown in Figure 40. Figures 41 and 42 show petrographic slides of the micaceous quartzose and volcanic lithic sandstones, respectively. Bedding ranges from thinly laminated to massive, with thin bedding more common in the micaceous quartzo-feldspathic sandstones and massive bedding more common in the volcanic lithic sandstone. An outcrop of crudely bedded volcanic lithic sandstone is shown in Figure 43. Cross-bedding was observed in one outcrop of fine quartzo-feldspathic sandstone. Vitric sandstone typical of the Troutdale Formation in the type section area was not observed.

Conglomerates were rarely observed, although they are noted in many water well logs (Figure 34). Most of the conglomerates observed were volcanic-lithic pebble conglomerate with a volcanic-lithic and feldspathic sand matrix. The clasts are moderately to well-rounded, and matrix- to clast-supported. Sample PDX-168 was one of the few conglomerates observed, and a hand specimen, petrographic image, and outcrop photo are presented in Figures 44, 45, and 46, respectively. This conglomerate had common diatom tests in the matrix. Pebble to cobble

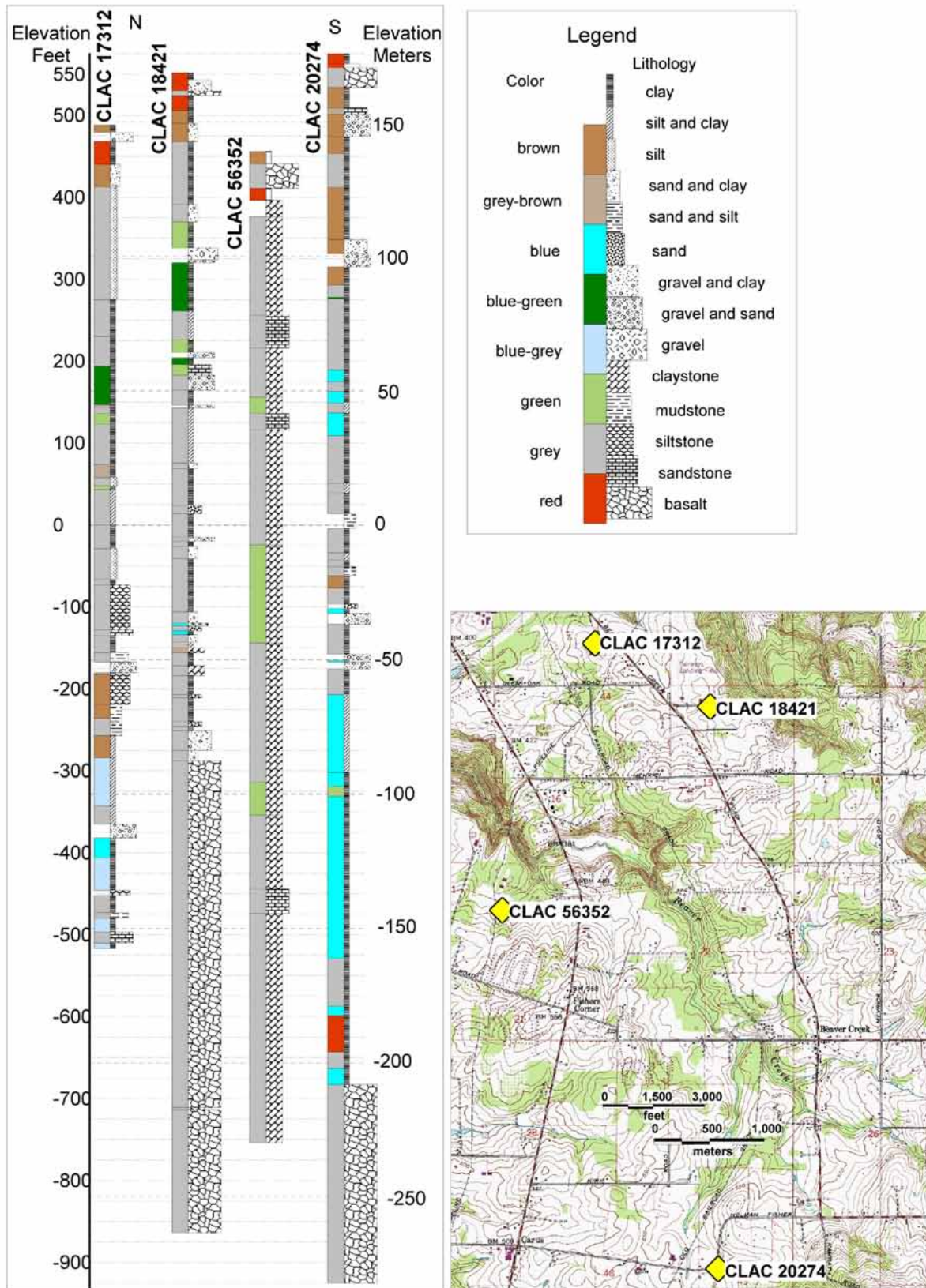


Figure 34. Troutdale Formation facies. Graphic logs of three deep water wells drilled in the Troutdale Formation. Note variability of lithology both between wells and within each well. Each well was logged by a different driller, which may account for some differences. Scale in feet.

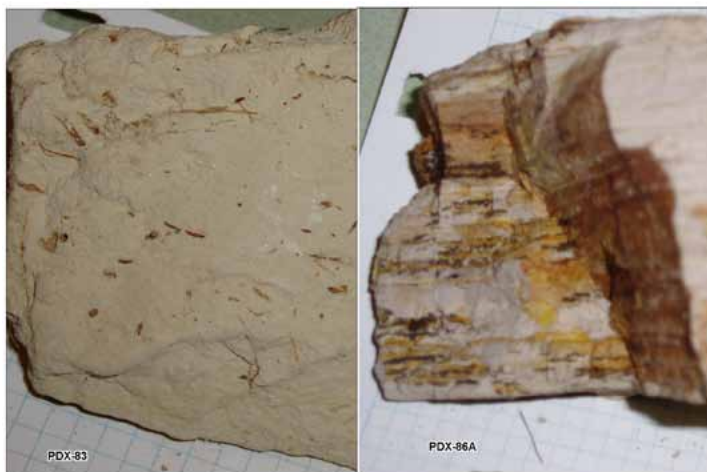


Figure 35. Hand specimens, Troutdale Formation mudstone. Grid on paper is 3 mm.

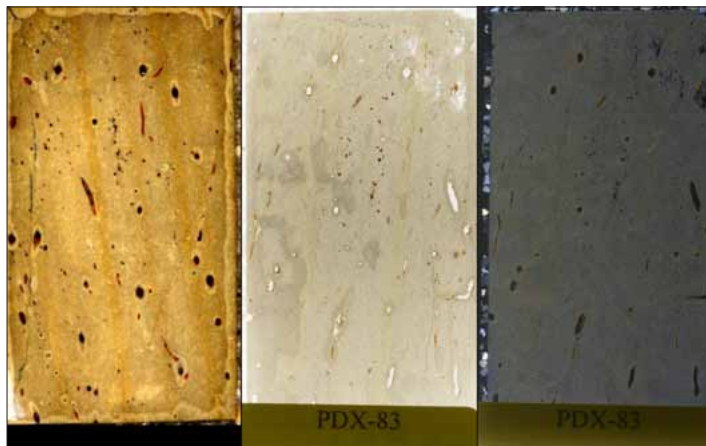


Figure 36. Petrography, Troutdale Formation mudstone (PDX-83). Scanned images of petrographic billet (left), slide in plane-polarized light (center), and slide in cross-polarized light (right). Images are 4.25 by 2.25 cm.

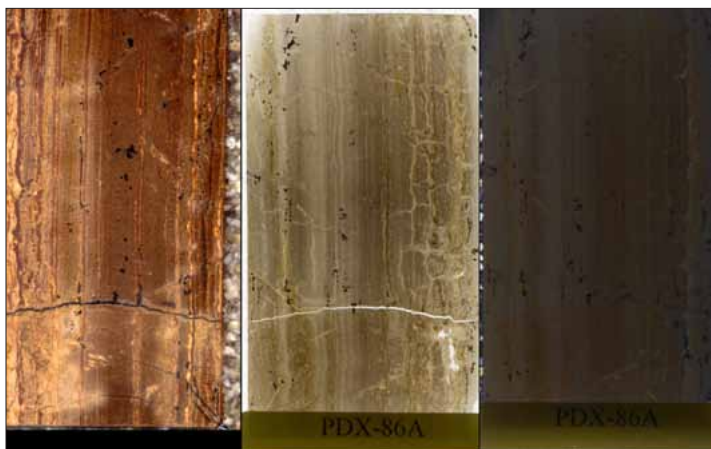


Figure 37. Petrography, Troutdale Formation mudstone (PDX-86A). Scanned images of petrographic billet (left), slide in plane-polarized light (center), and slide in cross-polarized light (right). Images are 4.25 by 2.25 cm.



Figure 38. Outcrop, Troutdale Formation laminated mudstone located at PDX-537. Field of view approximately 1 m wide.



Figure 39. Outcrop, Troutdale Formation massive mudstone. Hammer (center of photograph) for scale. No bedding was evident in the entire cut, located at PDX-74.

Figure 40. Hand specimens, Troutdale Formation sandstone. PDX-650 is volcanic-lithic sandstone, PDX-69A is micaceous quartzo-feldspathic sandstone. Grid on paper is 3 mm; pencil diameter is 6 mm.

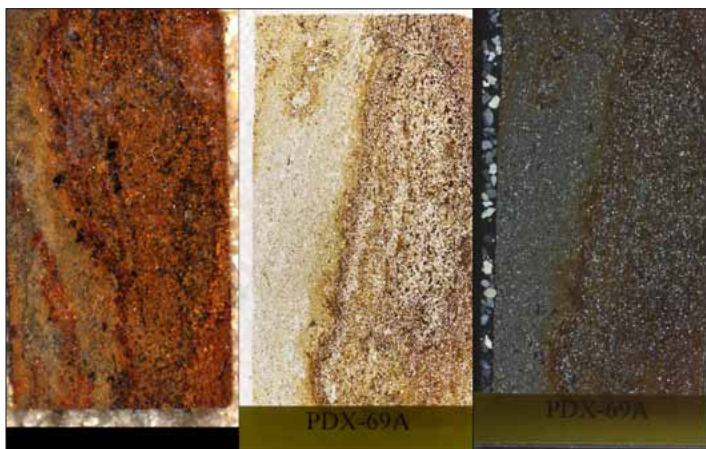


Figure 41. Petrography, Troutdale Formation micaceous quartzo-feldspathic sandstone (PDX-69A). Scanned images of petrographic billet (left), slide in plane-polarized light (center), and slide in cross-polarized light (right). Images are 4.25 by 2.25 cm.

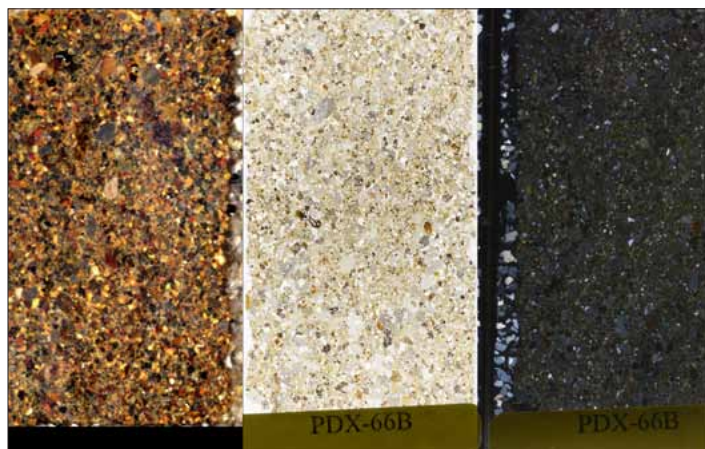


Figure 42. Petrography, Troutdale Formation volcanic-lithic sandstone (PDX-66B). Scanned images of petrographic billet (left), slide in plane-polarized light (center), and slide in cross-polarized light (right). Images are 4.25 by 2.25 cm.



Figure 43. Outcrop, Troutdale Formation volcanic lithic sandstone, located at PDX-332.



Figure 44. Petrography, Troutdale Formation conglomerate (PDX-168). Scanned images of petrographic billet (left), slide in plane-polarized light (center) slide in crossed polars (right). Images are 4.25 by 2.25 cm.

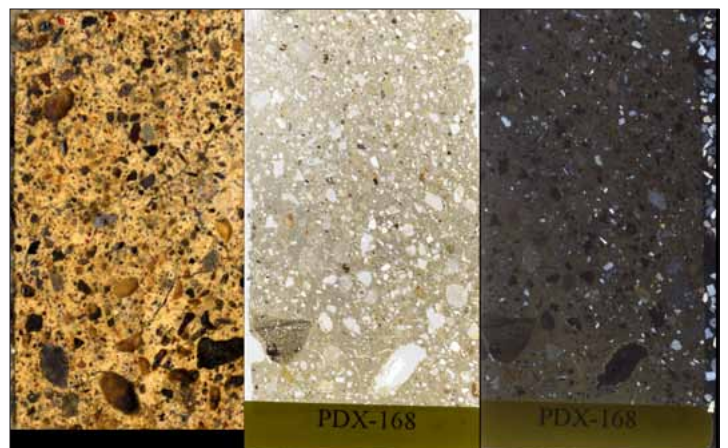


Figure 45. Petrography, Troutdale Formation conglomerate (PDX-168). Scanned images of petrographic billet (left), slide in plane-polarized light (center), and slide in cross-polarized light (right). Images are 4.25 by 2.25 cm.



Figure 46. Outcrop, Troutdale Formation conglomerate located at PDX-168.

quartz sandstones, quartzite cobble conglomerate) and from rivers draining the Cascade Range (volcanic lithic claystone, sandstone and conglomerate). This suggests that the depositional environment was a broad alluvial plain across which the paleo-Columbia and its Cascade Range tributaries migrated.

Columbia River Basalt Group

The oldest rocks exposed in the map area are the middle Miocene tholeiitic flood lavas of the Columbia River Basalt Group (CRBG). CRBG units in the quadrangle make up but a small part of the approximately 164,000 km² of the Pacific Northwest underlain by Columbia River Basalt flows; many individual flows were known to be huge in size, many covering thousands to tens of thousands of square kilometers in area, with volumes up to thousands of cubic kilometers (Tolan and others, 1989). These enormous flows erupted from vents in eastern Oregon and Washington and western Idaho and flowed through the Portland region on their way to the Pacific Ocean. Individual Columbia River Basalt Group units are defined on the basis of stratigraphic position, geochemistry, magnetic polarity, and petrography following the work of Swanson and others (1979), Reidel and others (1989), and Beeson and others (1985, 1989).

CRBG units exposed in the map area include the Sand Hollow and Ginkgo units of the Frenchman Springs Member of the Wanapum Basalt. Two additional units of this member, the basalt of Silver Falls and the basalt of Sentinel Gap, were reported from deep wells in the quadrangle (USGS, 2006; Appendix F) but not exposed at the surface. The Sentinel Bluffs Member of the Grande Ronde Basalt (Reidel, 2005) and the basalt of Winter Water of the same formation are also exposed.

Wanapum Basalt-Frenchman Springs Member

Twfs basalt of Sand Hollow (middle Miocene)—black basalt flows with sparse plagioclase phenocrysts (Figure 47). The basalt of Sand Hollow is exposed near the northwest corner of the map, where the basalt caps the ridge above West Linn; makes up the intermediate elevation slopes above Oregon City; and is exposed along the banks of the Willamette River on the downthrown side of the Bolton Fault. Another small exposure is present along the Bolton Fault at the east edge of the map in Section 13, T. 3. S., R. 2 E.

The basalt of Sand Hollow overlies the basalt of Ginkgo and is overlain by the Troutdale Formation.

The lava is typically black where fresh, weathering to dark grey or greenish grey. Plagioclase phenocrysts up to 3 mm long occur sparsely in some flows. The flows typically are typically columnar jointed.

Petrographically, the basalt is medium-grained and consists of plagioclase laths up to 1.5 mm long, subophitic to intergranular pyroxene up to 1.5 mm long, interstitial dark brown glass, and sparse elongate plagioclase phenocrysts up to 3 mm long (Figure 48).

Geochemically, the lavas are basalts (Figure 49) with high TiO₂ (average 3.07%), FeO (average 13.7%), and P₂O₅ (average 0.58%). The basalt of Sand Hollow is distinguished from the otherwise chemically very similar basalt of Ginkgo by higher Cr (average 40 ppm) and from the Grande Ronde Basalt by lower SiO₂ (average 51.6%) and higher TiO₂ (Figure 50). Geochemically analyzed samples are plotted on the map, and analytical data are provided in Appendix D.

The age of the basalt of Sand Hollow is middle Miocene on the basis of K-Ar date of 15.3 Ma reported by Beeson and others (1985).

The maximum thickness of the unit inferred for the map area is approximately 90 m (cross section B-B', Plate 1).

Twfg basalt of Ginkgo (middle Miocene)—black basalt flows with abundant plagioclase phenocrysts (Figure 51). The basalt of Ginkgo is exposed near the northwest corner of the map, where the basalt makes up much of the ridge above West Linn, underlies much of downtown Oregon City, and crops out along the Highway 43 in a fault sliver along the Bolton Fault. A small exposure is found along the Bolton Fault at the east edge of the map in Section 13, T. 3. S., R. 2 E.



Figure 47. Hand specimen, basalt of Sand Hollow (PDX-125). Grid on paper is 3 mm.

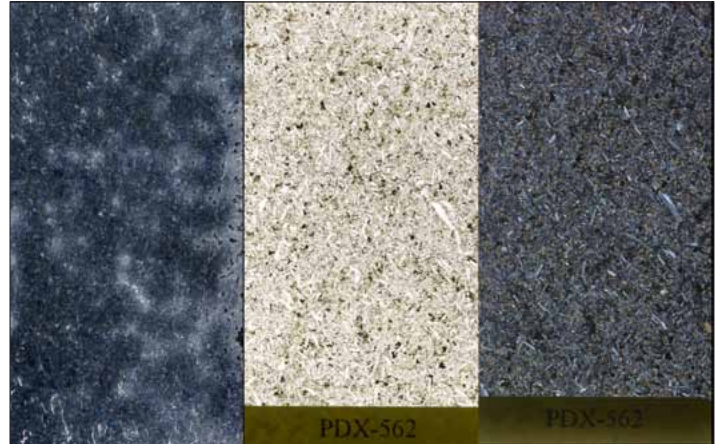


Figure 48. Petrography, basalt of Sand Hollow (PDX-562). Scanned images of petrographic billet (left), slide in plane-polarized light (center), and slide in cross-polarized light (right). Images are 4.25 by 2.25 cm.

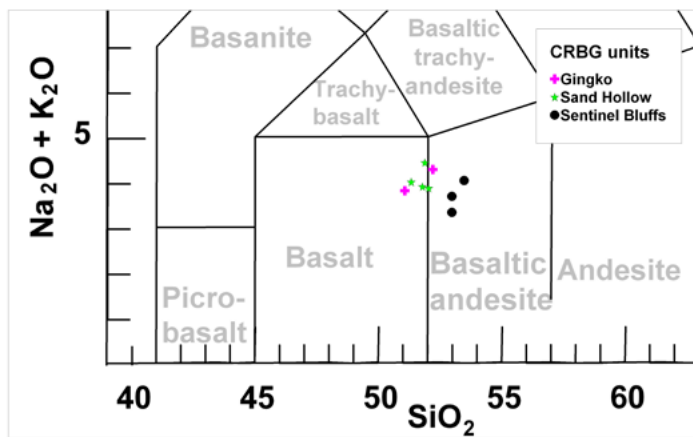


Figure 49. Columbia River Basalt Group lava composition. LeBas and Streckisen (1991) TAS diagram.

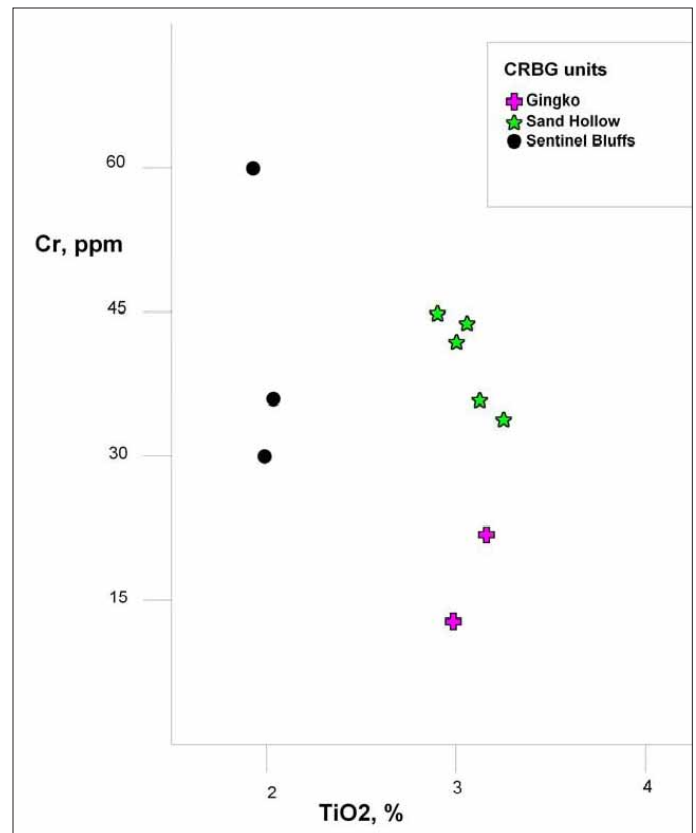


Figure 50. Columbia River Basalt Group unit Ti versus Cr plot.

The basalt of Ginkgo overlies the Sentinel Bluffs Member of the Grande Ronde Basalt and is overlain by the basalt of Sand Hollow.

The lava is typically dark gray or black where fresh, weathering to gray with a purplish brown surface. Plagioclase phenocrysts up to 15 mm and plagioclase glomerocrysts up to 20 mm long are common. The flows typically are blocky to columnar jointed, with columns 1 to 1.75 m in diameter common (Figure 52).

Petrographically, the basalt is medium-grained and consists of plagioclase laths up to 1.5 mm long, subophitic pyroxene up to 1.5 mm long, interstitial dark brown glass, and elongate plagioclase phenocrysts up to 15 mm long (Figure 53).

Geochemically, the lavas are basalts (Figure 50) with high TiO_2 (average 3.07%), FeO (average 14.2%), and P_2O_5 (average 0.67%). The basalt of Ginkgo is distinguished from the otherwise chemically very similar basalt of Sand Hollow by the lower Cr (average 17 ppm) and from the Grande Ronde Basalt by lower SiO_2 (average 51.6%) and higher TiO_2 (Figure 50). Geochemically analyzed samples are plotted on the map, and analytical data are provided in Appendix D.

The age of the basalt of Ginkgo is middle Miocene, because the basalt is overlain by the 15.3 Ma basalt of Sand Hollow and overlies the 15.6 Ma Basalt of Sentinel Bluffs.

The maximum thickness of the unit inferred in the map area is approximately 75 m (cross section B-B', Plate 1).

Grande Ronde Basalt

Tgsb Sentinel Bluffs Member (middle Miocene)—black basalt flows with sparse plagioclase phenocrysts (Figure 54). The Sentinel Bluffs Member is exposed in the northwest corner of the map, where it makes up most of the shoreline exposures along the Willamette River.

The Sentinel Bluffs Member overlies the basalt of Winter Water of the Grande Ronde Basalt and overlain by the basalt of Ginkgo.

The lava is typically dark gray or black where fresh, weathering to greyish brown. Sparse plagioclase phenocrysts up to 10 mm occur. The flows typically are blocky to platy jointed and are typically highly vesicular near the flow tops with horizontal bands of flattened vesicles and vugs (Figure 55). In excellent exposures along the Willamette River, the unit there are several thin lobes marked by thin breccia zones separating more massive rock.

Geochemically, the Sentinel Bluffs Member is a basaltic andesite (Figures 49 and 50) with lower TiO_2 (average 2%) and FeO (average 12.2%) and higher MgO (average 4.6%) and SiO_2 (average 53.1%) than the overlying Wanapum Basalt. Geochemically analyzed samples are plotted on the map, and analytical data are provided in Appendix D.

The upper part of the Sentinel Bluffs Member is marked by a highly vesicular and deeply weathered zone that is typically red-brown. The weathered zone is overlain by a thin (0.7 to 1.5 m) deposit of claystone or sandstone. This sediment is correlated to the Vantage Member of the Ellensburg Formation (Swanson and others, 1979; Beeson and others, 1985) and in the map area is a tan medium-grained micaceous quartz sandstone (Figure 56). The contact between the Grande Ronde Basalt and Wanapum Basalt is also responsible for Willamette Falls, where the river cascades over the top of the Sentinel Bluffs Member (Figure 57).

The age of the Basalt of Sentinel Bluffs is middle Miocene, with a reported $^{40}\text{Ar}/^{39}\text{Ar}$ date of approximately 15.6 Ma for the youngest flows of this unit on the Columbia Plateau (Long and Duncan, 1982).

The exposed thickness of the unit in the map area is approximately 45 m.

Tgww basalt of Winter Water (middle Miocene)—flow or flows of basaltic andesite. The basalt of Winter Water was not observed by the author, but Terry L. Tolan (personal communication, 2005) reports several exposures in the area along the northwest shore of the Willamette River and at the south end of Highway 43. The basalt of Winter Water is widely exposed on the adjacent Lake Oswego quadrangle, where the basalt is described by Beeson and others (1989) as dark gray to black where fresh, greenish grey to grayish black where weathered, glassy to fine grained, and phyrlic to abundantly phyrlic with small (less than 3 mm) plagioclase glomerocrysts that often display a distinctive radial habit. It is distinguished from the overlying Sentinel Bluffs Member by the presence of phenocrysts and by higher TiO_2 and lower MgO.



Figure 51. Hand specimen, basalt of Gingko (PDX-124). Grid on paper is 3 mm.

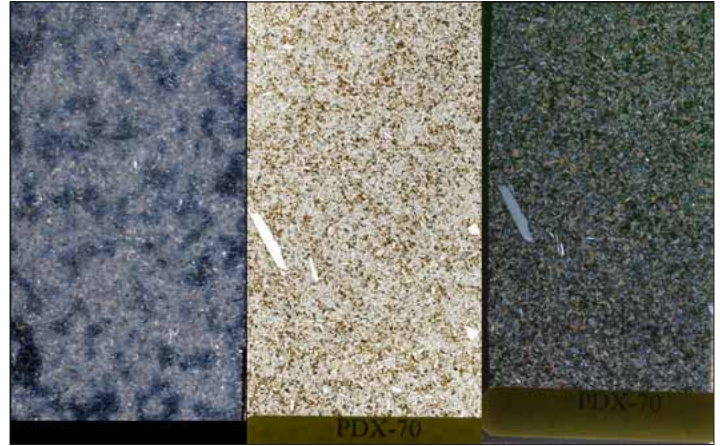


Figure 53. Petrography, basalt of Gingko (PDX-70). Scanned images of petrographic billet (left), slide in plane-polarized light (center), and slide in cross-polarized light (right). Images are 4.25 by 2.25 cm.



Figure 52. Outcrops, basalt of Gingko (left, PDX-124; right, PDX-122). Note abundant coarse plagioclase phenocrysts in PDX-124, large columns in PDX-122.



Figure 54. Hand specimen, Sentinel Bluffs Member (PDX-123). Grid on paper is 3 mm.



Figure 56. Hand specimen, Vantage Member sandstone of the Ellensburg Formation (PDX-138). Grid on paper is 3 mm.



Figure 55. Outcrops, Sentinel Bluffs Member. Note horizontal bands of flattened vugs and vesicles, located at PDX-123.



Figure 57. Willamette Falls. The Willamette River plunges 14 m over the top of the uppermost flow of the Sentinel Bluffs Member of the Grande Ronde Basalt. The cliffs in the background of the photograph are coarse columns of the overlying Ginkgo flow of the Frenchman Springs Member of the Wanapum Basalt. The flow of the Willamette River at the time of the photograph was $471 \text{ m}^3/\text{s}$. Peak recorded discharge was $8,085 \text{ m}^3/\text{s}$. As much as 250 cubic kilometers of water flowed past this site to fill the Willamette Valley during the largest Missoula floods. If one of the largest floods had taken a week to fill the valley, the average flow would have been $413,000 \text{ m}^3/\text{s}$, over 50 times the peak recorded flow. The falls probably originated 1,500 m downstream at the Bolton Fault and has migrated upstream, with the majority of migration probably accomplished during the Missoula floods.

Tcu Columbia River Basalt, undifferentiated (middle Miocene)—Shown only in cross section on the map plate.

STRUCTURE

Near the northwestern corner of the map, essentially flat-lying flows of the CRBG form the southeastern end of the 2 to 3 km wide Rosemont Ridge (informally named for a small community on the adjacent Lake Oswego quadrangle) that extends northwest for 8 km at an elevation of 180 to 225 m into the adjacent Lake Oswego quadrangle (Figure 58). The geology of this ridge consists of CRBG flows and minor loess cover. There is no evidence that the area was ever covered by the Troutdale Formation. Across the Willamette River to the southeast, the informally named Oregon City Plateau extends across the Oregon City quadrangle and ranges in elevation from about 120 m near the Willamette River to about 180 m in the southeastern corner. On the Oregon City Plateau, the CRBG is covered by as much as 300 m of flat-lying younger sedimentary and volcanic rocks.

Although these domains have very different geology, there is no major structure separating them. A combination of minor northeast-trending, southeast-side-down faults and a modest southeast dip of about 3 degrees combine to step the uppermost CRBG flows down about 100 m between the Rosemont Ridge and Oregon City Plateau. This structure, coupled with the erosion of the valley of Willamette River, accounts for the change in geologic domains.

The most important structures in the map area are the northwest-trending Bolton, Portland Hills, and Oatfield faults (Figure 58).

Bolton Fault

The Bolton Fault is the westernmost of the major faults and extends 12 km from one edge of the quadrangle to the other. The fault was originally mapped and named on the adjacent Lake Oswego quadrangle by Beeson and others (1989). The fault plane was not observed on the Oregon City quadrangle, and there is no obvious surface trace of the fault. Topographic expression is limited to the linear northeastern edge of the Rosemont Ridge. The fault is defined by abrupt changes in the elevation of CRBG unit contacts northwest of the Willamette River and by abrupt changes of the elevation of the base of the basalt of Canemah to the southeast. It should be noted that the base of the basalt of Canemah has considerable relief, making precise measurement of the offset of this unit difficult. Vertical offset of the CRBG units, as measured in cross section A-A' (Plate 1) is approximately

225 m, which, combined with the 15.6 to 15.3 Ma age of the flows and assuming a constant long-term slip, yields an approximate vertical slip rate of 0.015 mm/yr. Vertical offset of the basalt of Canemah as measured in cross section B-B' (Plate 1) is 55 m; measured farther southeast near Henrici Road where the contacts are best defined the offset is 28 m. The reported ages of the basalt of Canemah are 2.5 and 2.4 Ma. This yields an approximate slip rate of 0.011 to 0.022 mm/yr with the preferred rate of 0.011 mm/yr (28 m offset in 2.45 million years). The similarity between the slip rate derived from the CRBG and the Boring Lava suggests that deformation has been ongoing since the middle Miocene, with a possibility of marginally higher rates during the Quaternary.

There is contradictory evidence for horizontal slip along the Bolton Fault. Along the east edge of the map, the fault appears to truncate a north-trending valley-filling flow of the basaltic andesite of Beaver Creek (Figure 59). On the Redland quadrangle to the east, water well data and limited geochemical analyses define a north-trending valley-filling flow with similar dimensions and chemistry that is truncated on the south edge by the Bolton Fault. If these two flows are the same valley-filling flow, then there is approximately 2.5 km of right lateral offset. The age of the basaltic andesite of Beaver Creek is 2.6 Ma, which yields a horizontal slip rate of 1.0 mm/yr. This rate is much higher than any ever proposed for Portland area faults and is inconsistent with the lack of a surface trace for the fault. Either the two valley-filling flows are different, or the age of the basalt is much greater than 2.6 Ma. Lidar imagery of fault trace suggests that horizontal slip rates are at least as low as the vertical rates. Figure 60 shows a high-resolution lidar image (pixel size 1 m) of the area of the fault trace where it juxtaposes Troutdale Formation mudstone against the basalt of Canemah. Several small linear gullies cross the fault at right angles and show no horizontal offset, nor is there any apparent scarp due to vertical offset. The gullies change character slightly as they cross the fault, probably reflecting the change from mudstone uphill to basalt downhill.

One other feature of note along the Bolton Fault is the small outcrop of CRBG at the far eastern edge of the map. From limited exposures and well data this exposure is inferred to be a structural high uplifted along the Bolton Fault.

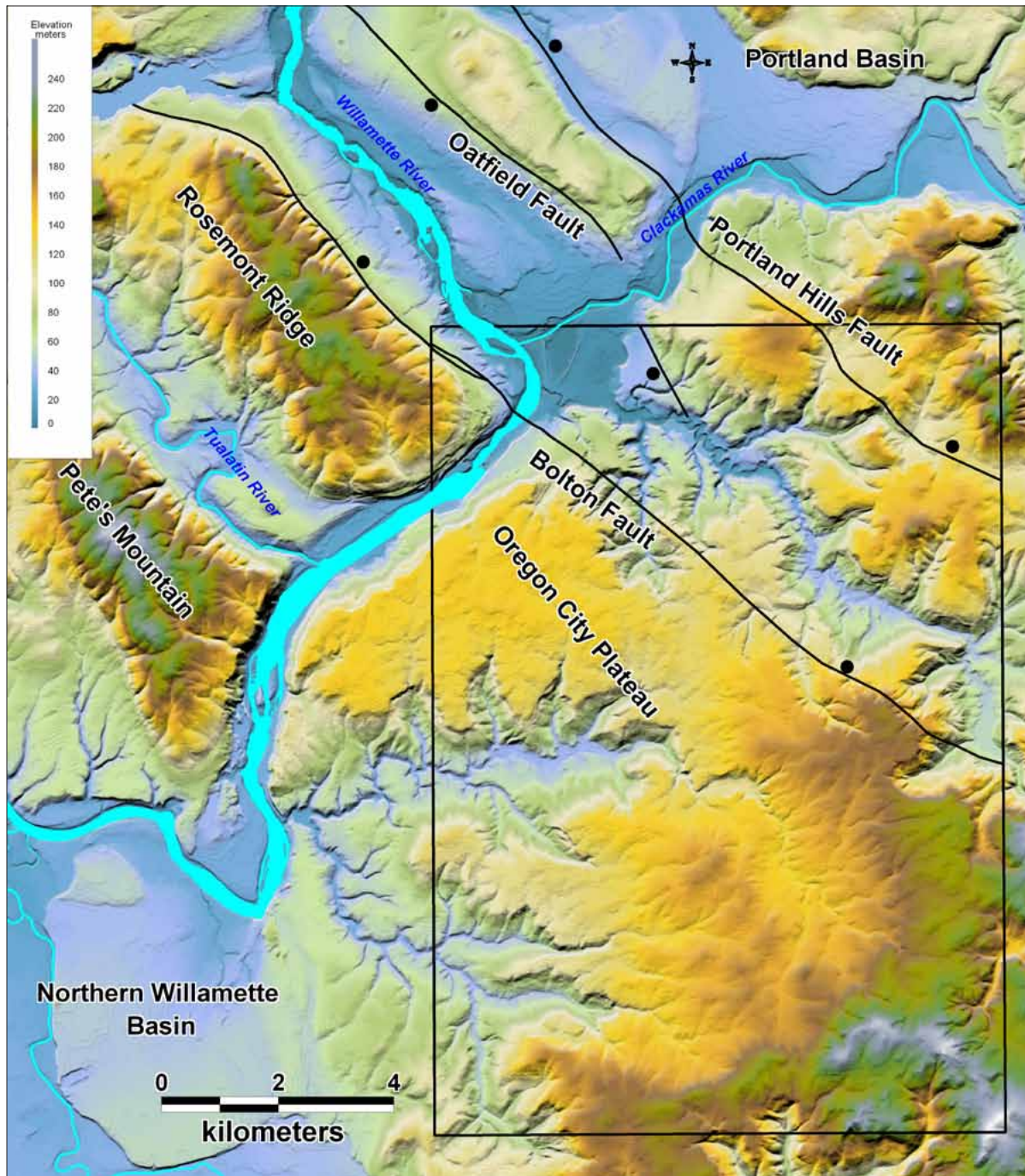


Figure 58. Regional landforms and structures. Heavy black box is the Oregon City quadrangle; heavy black lines are major faults, ball on downthrown side.

Portland Hills Fault

Madin (1990) mapped the Portland Hills Fault on the adjacent Gladstone (north) quadrangle largely from water well data. From field relationships and water well data the Portland Hills Fault is inferred to extend across the northeastern corner of the Oregon City quadrangle. In general, the evidence consists of abrupt changes in lithology, thickness of units, or elevations of contact surface mapped by well data, but it is important to note that the channel-filling nature of both sedimentary and volcanic units in the area could cause similar relationships. There is no direct evidence for the fault in the form of clearly offset contacts, surface trace, or exposure of the fault plane.

The fault is inferred to offset the basaltic andesite of Hunsinger (Plate 1, cross section C-C') approximately 90 m vertically, down to the northeast. Combined with the approximate age of the basaltic andesite of Hunsinger (1.2 Ma), this yields a vertical slip rate of 0.075 mm/yr, which is substantially higher than the slip rate for the Bolton Fault, but much more poorly constrained. There is no evidence for horizontal slip of the Portland Hills Fault in the Oregon City quadrangle.

Oatfield (?) Fault

Along the north edge of the map, between the Bolton Fault and the Portland Hills Fault, water well data suggest that the top of the CRBG in the subsurface rises sharply in elevation (Plate 1, cross section B-B'). An inferred fault has been mapped here, with southwest-side-down displacement, that is on strike with the Oatfield Fault in the Gladstone quadrangle. The southernmost end of the mapped Oatfield Fault extends to within 1 km of the Oregon City quadrangle. The Oatfield Fault is a major structure that extends at least 16 km along the west side of the Portland Hills with west-side-down displacement (Beeson and others, 1989, 1991; Madin 1990). No direct evidence for the fault exists on the Oregon City quadrangle; there are no offset contacts, surface traces, or exposures of the fault plane.

Minor Faults

Several minor faults occur on the quadrangle. Near the northwest corner, there is a small northeast-trending fault that offsets CRBG stratigraphy approximately 40 m down to the southeast. This fault is the continuation of one mapped by Beeson and Tolan (manuscript in preparation) on the adjacent Canby quadrangle.

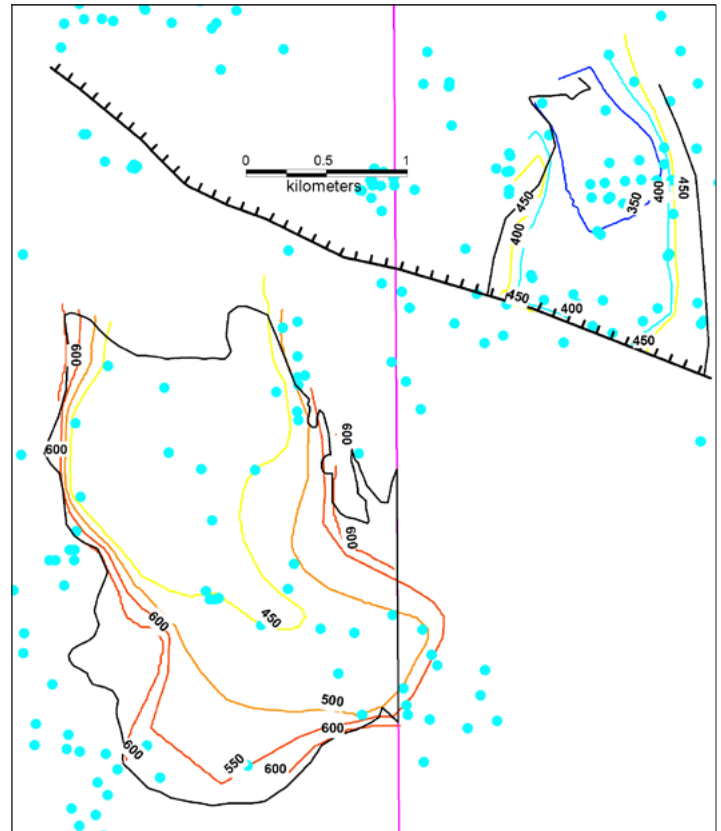


Figure 59. Horizontally offset (?) valley-filling flow. Vertical line in center is the eastern edge of Oregon City quadrangle; black lines are the edges of basaltic andesite of Beaver Creek (Tbb) chemistry flows; colored lines are structure contours on the base of the flows derived from water well data (blue dots). Hatched black line is the Bolton Fault.

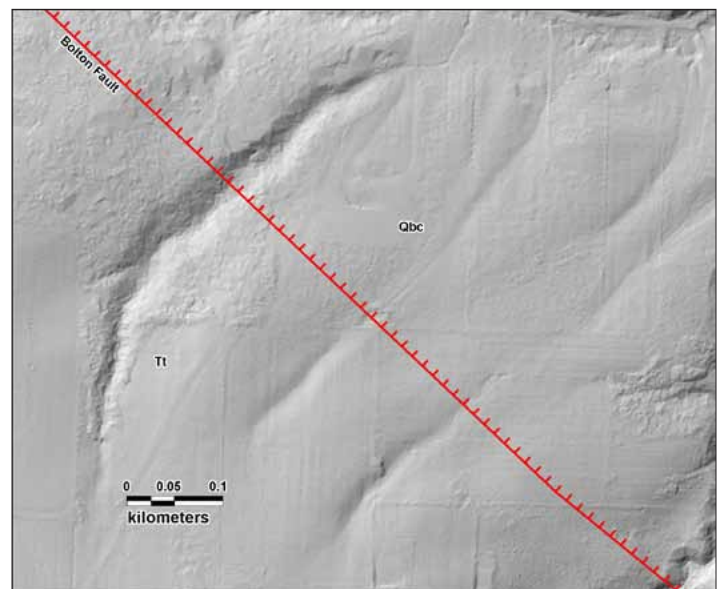


Figure 60. Lidar image of area of inferred trace of the Bolton Fault. Red hatched line is mapped fault, ticks on downthrown side. Bedrock on downthrown side is basalt, on upthrown side is mudstone. Located in Section 10, T. 3 S., R. 2 E.

In the northeast corner of the map there is a minor north-trending fault with west-side-down displacement of several tens of meters. This fault is a continuation of one mapped on the adjacent Gladstone quadrangle (Madin, 1990), where the fault was identified on the basis of abrupt changes in lithology. No direct evidence for the fault exists on the Oregon City quadrangle; there are no offset contacts, surface traces, or exposures of the fault plane.

Near the southwest corner of the map, a minor north-west-trending fault cuts the basalt of Canemah with north-east-side-down displacement. The evidence for the fault is the apparent offset of the base of the basalt, determined from water well data. There is no surface trace of the fault, nor was the fault plane exposed. There are approximately 30 m of vertical offset of the basalt, which gives a slip rate of 0.012 mm/yr.

RESOURCES

Geologic resources present in the Oregon City quadrangle include sand and gravel, basalt for aggregate, diatomite, and groundwater. None are currently being exploited, and only sand and gravel have any history of use.

Sand and gravel from the Quaternary alluvium have been mined for aggregate in the north of the map area along the Clackamas River. A pond now fills the quarry. Small quarries in Boring volcanic field rocks also produced minor rock, including one quarry in the basalt of Canemah at Water Board Park, and another in the basaltic andesite of Hunsinger near the vent for that unit. The CRBG has not been exploited for rock within the quadrangle. Considerable additional rock resources remain in the area, largely in the form of thick flows of the Boring volcanic field.

Some Troutdale Formation mudstones have high diatom contents, but the deposits are probably too impure, thin, and discontinuous, and they have not been mined. Groundwater is widely used for domestic water supplies outside the areas served by municipal water systems. A few large nurseries and golf courses irrigate with groundwater. In general, domestic wells are 30–90 m deep and produce modest amounts of water from thin sand and gravel beds in the Troutdale Formation. A few deep wells produce water from the Columbia River Basalt. Figure 61 shows the distribution of reported yield from located wells used for this study. There is an interesting band of high yield parallel to and

southwest of the Bolton Fault, and another subparallel band of lower yield further south. As most of these wells produce from the Troutdale Formation it is not clear what the origin of this anomaly is. Elsewhere in the quadrangle, anomalies in the yields have little pattern relative to geology, and many highs and lows are driven by a single well. Well construction and testing techniques vary widely, so there is much noise in the spatial patterns of yield.

Figure 62 shows the depth to first water throughout the map area. Again there is a band of anomalously shallow water parallel to and southwest of the Bolton Fault and another band of deep water yet farther southwest, closely mimicking the pattern of the yield map. This may be due to ponding of groundwater against the Bolton Fault. Elsewhere in the map, there is fair correlation between increased depth to first water and the presence of basaltic andesite units, probably because these flows are typically thick and massive. As with the yield maps, measurement of first water varies greatly from driller to driller; hence many strong anomalies are due to single wells.

Figure 63 shows the depth to the static water level in completed wells (measured at construction). Although the dominant pattern is that the static water level mimics the topography, there is a pronounced gradient across the Bolton Fault, again suggesting that the fault is relatively impermeable to groundwater flow.

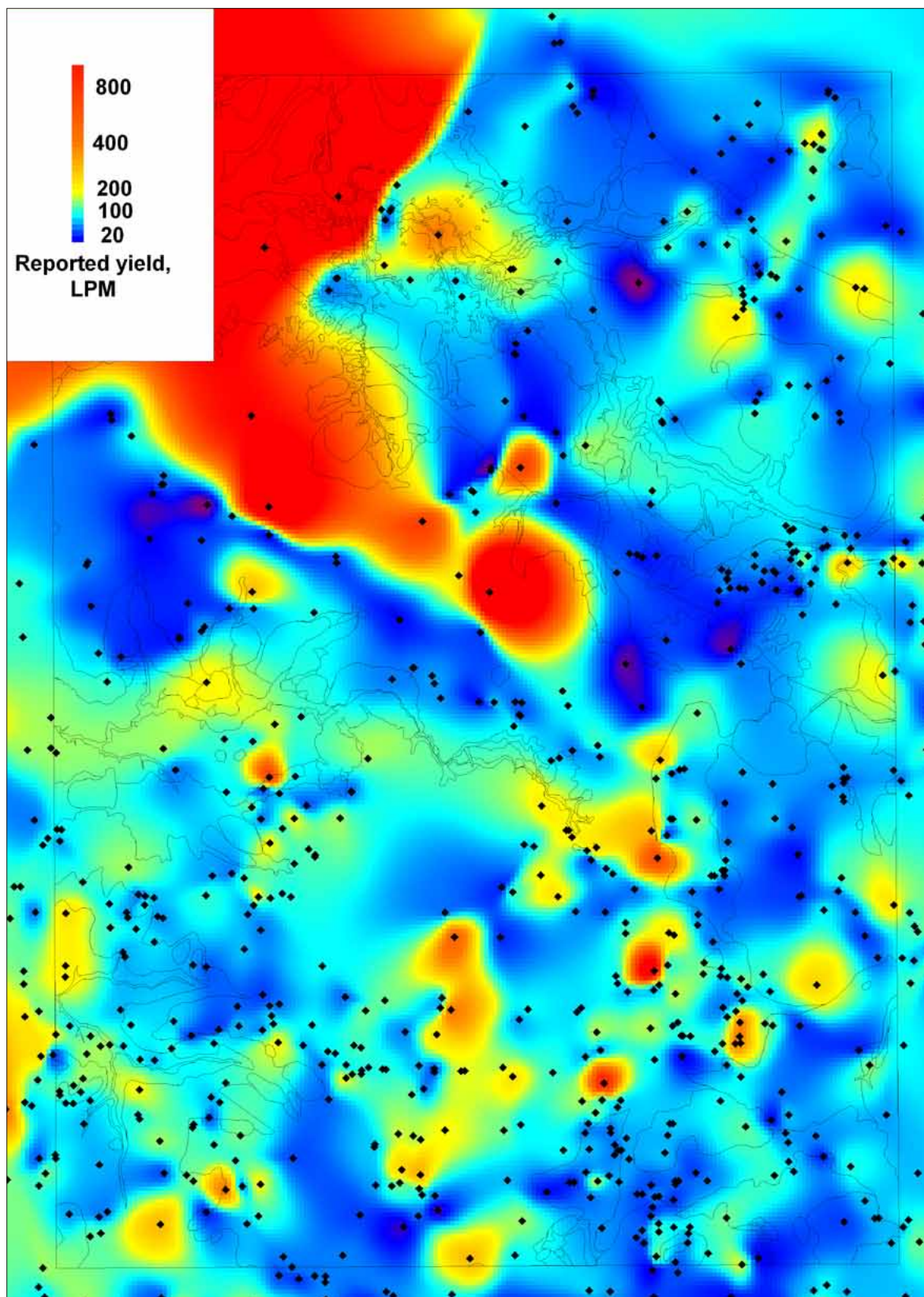


Figure 61. Well yield data. Reported well yield in gallons per minute, gridded at 50-m cells. Points show wells used; black lines are geology polygons.

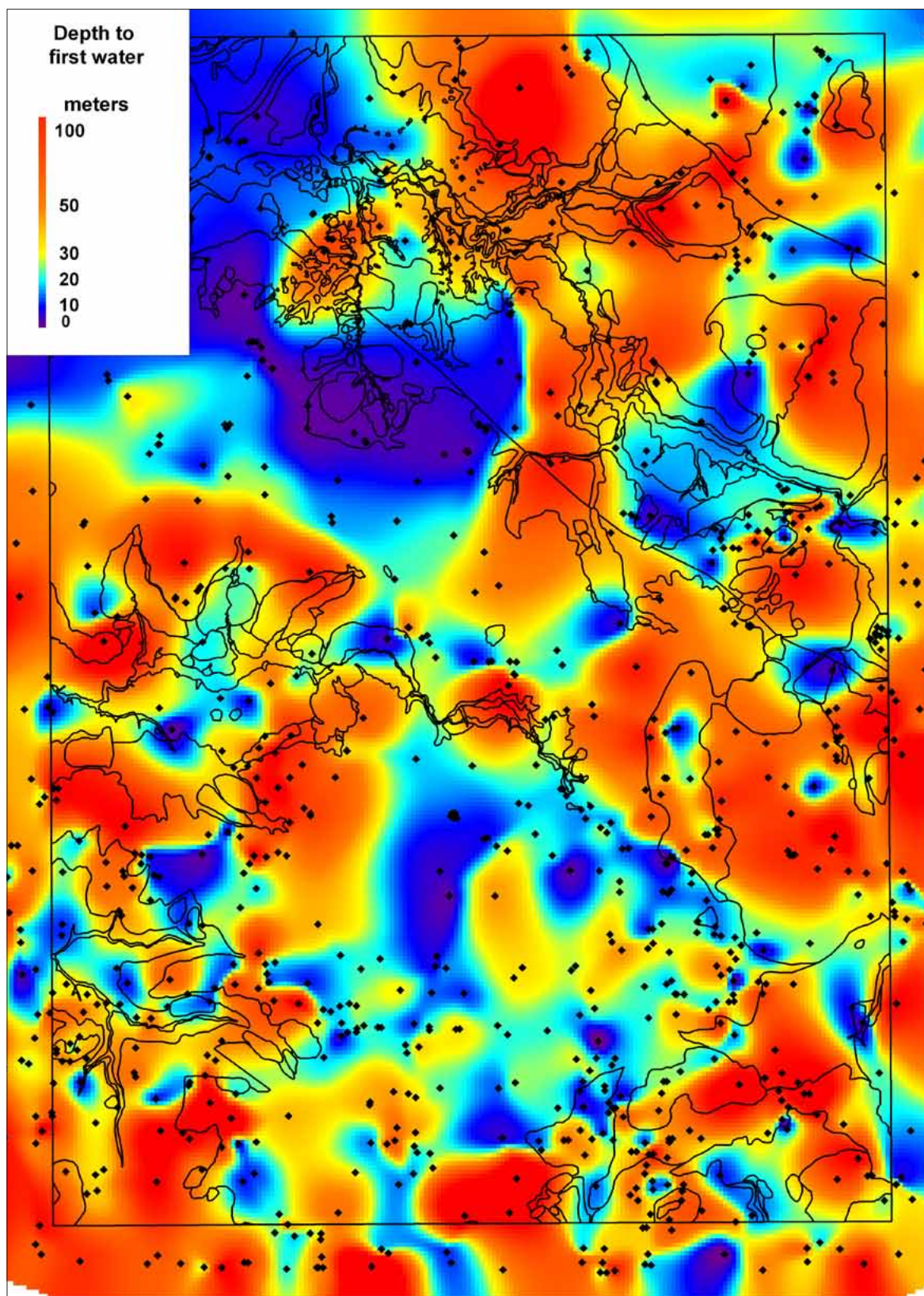


Figure 62. First water. Reported depth to first water in feet gridded at 50-m cells. Points show wells used; black lines are geology polygons.

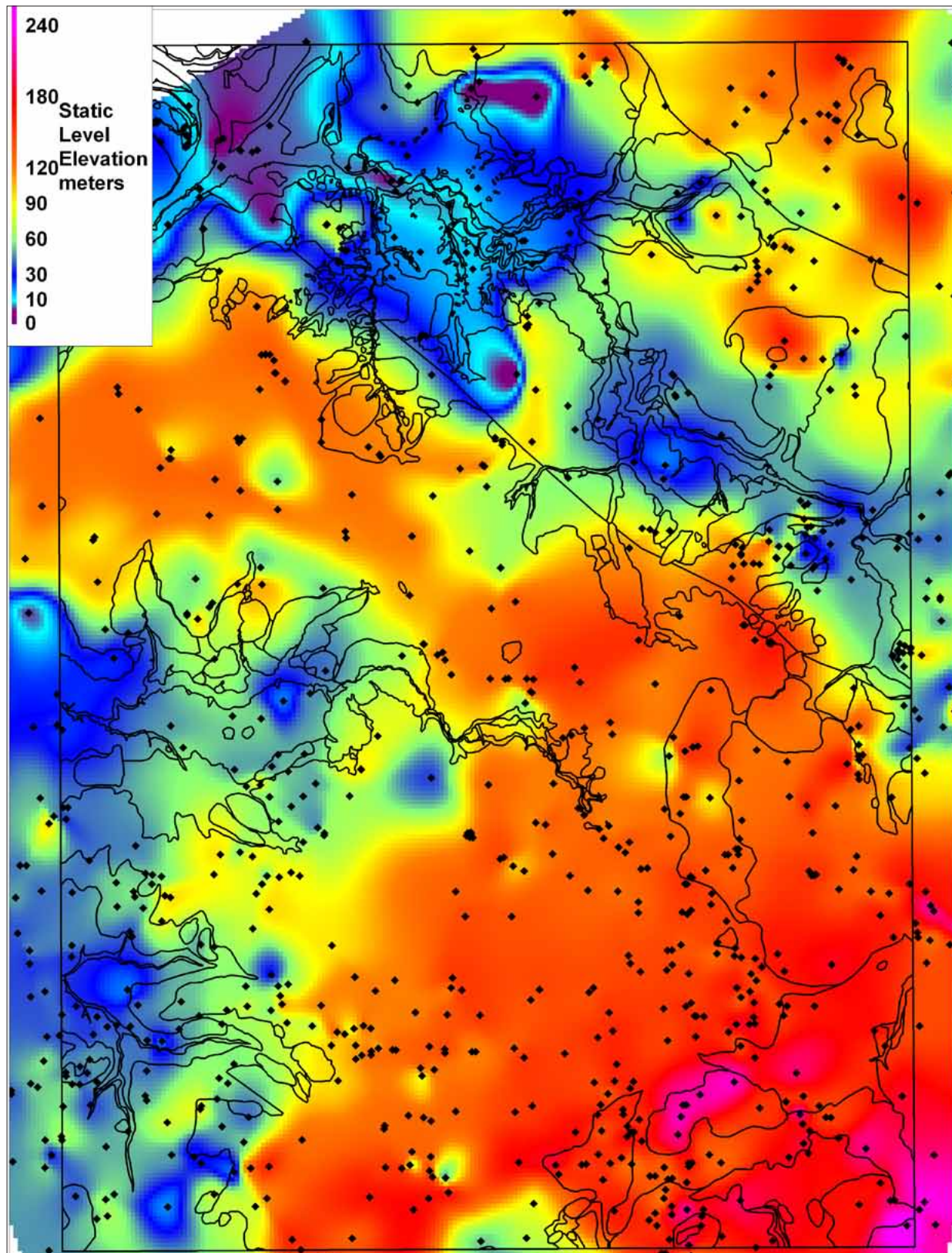


Figure 63. Static water level. Reported elevation (feet) of water table gridded at 50-m cells. Points show wells used; black lines are geology polygons.

HAZARDS

The dominant geologic hazards in the study area are landslides, earthquakes, floods, and stream erosion.

Flooding and minor stream bank erosion are to be expected along the floodplains of the many minor streams that feed into Abernethy and Beaver creeks, as the banks are typically composed of fine-grained young alluvium. Development changes associated with the expansion of the City of Oregon City may increase storm runoff by adding impermeable surfaces and storm drainage the feeds to local streams. Given the size of the basin, flooding on the Willamette River is controlled by regional events, but erosion effects in the map area are likely to be minimal along the Willamette as most of its banks are either bedrock or riprap.

Earthquake hazards in the area are modest, with most of the threat of ground shaking coming from offshore subduction zone earthquakes and from random local events in the M 5–6.5 range. Frankel and others (1997) calculated that the peak ground acceleration that has a 10% chance of being exceeded in the next 50 years ranges from 16 to 18% of g (acceleration due to gravity) for the quadrangle. The strength of shaking that has only a 2% chance of being exceeded in the next 50 years ranges from 33 to 39% of g .

Local earthquakes originating on the Bolton or Portland Hills faults are possible within the map area, although the slip rates for both faults are very low and suggest recurrence intervals for damaging earthquakes on the order of tens of thousands of years. There is a risk of fault rupture hazard along the traces of the Bolton and Portland Hills faults, but as the rate of activity on both is so low that there is no visible surface trace, the risk is likely very small and is very difficult to accurately locate.

Landslides represent the dominant hazard in the map area and come in two general classes. Large, deep-seated block

slides cover up to tens of hectares and extend to depths of tens of meters. Smaller, rapidly moving slides accompany intense rainfall events and may originate from failures only a few tens of square meters in size, but the debris generated may run downslope and down stream channels for significant distances with damaging force.

Landslides were mapped in this study by examination of historical air photos and lidar images to find areas of distinctive landslide topography. A small number of slides were actually identified in the field, again on the basis of distinctive topography. Burns (1999) performed a more detailed study of Newell Canyon in the northwest quarter of the map and found far more landslides during extensive fieldwork. Burns (1999) concluded that the shallow-seated slides were the dominant form of mass wasting in the Newell Canyon study area and that they often produced small debris flows.

The geology of Newell Canyon is similar to that of other canyons in the map area. It is likely that a similar landslide regime is common, with frequent shallow failures of loose fine-grained soil and weathered bedrock, and rare large deep-seated slides that cover many hectares. Neither condition necessarily precludes development, but development on or near steep slopes or on mapped slides should proceed only after site-specific evaluation by a registered geologist, engineering geologist, or geotechnical engineer. Schlicker and Finlayson (1979) depicted landslide hazard zones that are largely in accord with the results of this study.

Madin and Burns (2006) prepared a detailed lidar-based map of all landslides within the greater Oregon City area (see lidar coverage, Figure 3). Where that study and this study overlap, landslide polygons are identical.

GEOLOGIC HISTORY

The geologic history of the area begins with the middle Miocene eruption of the lava flows of the CRBG from vents in eastern Oregon and Washington. These enormous flows traveled hundreds of kilometers to the Portland area and covered the existing terrain with a stack of flows up to hundreds of meters thick. In the Oregon City quadrangle these flows buried older volcanic rocks of the Eocene basalt of Waverly Heights, exposed beneath the CRBG on the Lake Oswego and Canby quadrangles.

After eruption of the CRBG ceased, the ancestral Columbia River and local streams began to deposit fluvial sediments of the Troutdale Formation in the slowly subsiding Portland Basin. The absence of Troutdale Formation on the Rosemont Ridge (Figure 58) suggests that some uplift along the Bolton Fault may have predated deposition of the Troutdale Formation.

Deposition of the Troutdale Formation continued into the late Pliocene, when local faulting and Boring volca-

nic field volcanism began in the Portland Basin (Madin, 1994). During the late Pliocene and Pleistocene, the ancestral Clackamas River and its tributaries carved canyons through the Troutdale that filled with Springwater Formation and with flows of lava from the Boring volcanic field vents. Many of the vents developed into small volcanoes that are visible today.

During the late Pleistocene, catastrophic Missoula floods repeatedly swept the area, inundating the lowlands and filling the canyons. The floods scoured the Willamette River channel and basalt bedrock in West Linn and Oregon City; in backwater areas, tens of meters of flood sand and silt were deposited.

After the floods, local streams re-established their courses through the flood deposits, cutting terraces and depositing floodplain alluvium in the process.

During the late Pleistocene and Holocene, widespread landslide failures, many of which remain active, occurred in steep canyons.

Acknowledgments

Russell Evarts of the USGS and Richard Conrey of Washington State University conducted a parallel study of the Boring volcanic field during the time of this project and provided invaluable geochemical analytical data and advice.

Detailed review was provided Terry Tolan of Kennedy/Jenks consultants; Russell Evarts of the USGS; and Vicki McConnell, Oregon Department of Geology and Mineral Industries. Lidar imagery was provided courtesy of the City of Oregon City and the Portland Lidar Consortium.

Research was supported by the USGS, Department of the Interior, under USGS award 03HQAG0013. The views and conclusions contained in this document are those of the author and should not be interpreted as necessarily representing the official policies, either expressed or implied, of the U.S. Government.

REFERENCES

- Allen, J. E., Burns, M., and Sargent, S. C., 1986, *Cataclysms on the Columbia: Portland, Oregon*, Timber Press, 211 p.
- Baker, V. R., and Nummedal, D., eds., 1978, *The channeled scabland: Washington, D.C.*, National Aeronautics and Space Administration, 186 p.
- Beeson, M. H., and Tolan, T. L., in preparation, *Geologic map of the Canby 7.5' quadrangle, Clackamas county, Oregon: U.S. Geological Survey Miscellaneous Field Studies*, scale 1:24,000.
- Beeson, M. H., Fecht, K. R., Reidel, S. P., and Tolan, T. L., 1985, Regional correlations within the Frenchman Springs Member of the Columbia River Basalt Group: New insights into the middle Miocene tectonics of northwestern Oregon: *Oregon Geology*, v. 47, no. 88, p. 87–96.
- Beeson, M. H., Tolan, T. L., and Madin, I. P., 1989, *Geologic map of the Lake Oswego quadrangle, Clackamas, Multnomah, and Washington counties, Oregon: Oregon Department of Geology and Mineral Industries Geologic Map Series 59*, scale 1:24,000.
- Beeson, M. H., Tolan, T. L., and Madin, I. P., 1991, *Geologic map of the Portland quadrangle, Multnomah and Washington counties, Oregon: Oregon Department of Geology and Mineral Industries Geologic Map Series 75*, scale 1:24,000.
- Benito, G., and O'Connor, J. E., 2003, Number and size of last-glacial Missoula floods in the Columbia River valley between the Pasco Basin, Washington, and Portland, Oregon: *GSA Bulletin*, v. 115, no. 5, p. 624–638.
- Bretz, J. H., Smith, H. T. U., and Neff, G. E., 1956, Channeled scabland of Washington: New data and interpretations: *Geological Society of America Bulletin*, v. 67, no. 8, p. 957–1049.
- Burns, W. J., 1999, *Engineering geology and relative stability of the southern half of Newell Creek canyon, Oregon City, Oregon: Portland, Ore., Portland State University, M.S. thesis*, 143 p., 3 pl.
- Conrey, R. M., Uto, K., Uchiumi, S., Beeson, M. H., Madin, I. P., Tolan, T. L., and Swanson, D. A., 1996, Potassium-argon ages of Boring Lava, northwest Oregon and southwest Washington: *Isochron West*, no. 63, p. 3–9.
- Fleck, R. J., Evarts, R. C., Hagstrum, J. T., and Valentine, M. J., 2002, The Boring volcanic field of the Portland, Oregon area—geochronology and neotectonic significance: *Geological Society of America Abstracts with Program*, v. 33, no. 5, p. 33–34.
- Frankel, A., Mueller, C., Barnhard, T., Perkins, D., Leyendecker, E. V., Dickman, N., Hanson, S., and Hopper, M., 1997, *Seismic-hazard maps for the conterminous United States, Map F—Horizontal spectral response acceleration for 0.2 second period (5% of critical damping) with 2% probability of exceedance in 50 years: U.S. Geological Survey Open-File Report 97-131-F*.
- Frankel, A. D., Petersen, M. D., Mueller, C. S., Haller, K. M., Wheeler, R. L., Leyendecker, E. V., Wesson, R. L., Harmsen, S. C., Cramer, C. H., Perkins, D. M., and Rukstales, K. S., 2002, *Documentation for the 2002 update of the national seismic hazard maps: U.S. Geological Survey Open-File Report 02-420*, 33 p.
- Hofmeister, R. J., 2000, *Slope failures in Oregon: GIS inventory for three 1996/97 storm events: Portland, Ore., Oregon Department of Geology and Mineral Industries Special Paper 34*, 20 p.
- Johnson, D. M., Hooper, P. R., and Conrey, R. M., 1999, XRF analysis of rocks and minerals for major and trace elements on a single low dilution Li-tetraborate fused bead: *Advances in X-ray Analysis*, v. 41, p. 843–867.
- Le Bas, M. J., and Streckeisen, A. L., 1991, The IUGS systematics of igneous rocks: *Journal of the Geological Society*, v. 148, p. 825–833.
- Lite, K. E. Jr., 1992, *Stratigraphy and structure of the southeast part of the Portland Basin, Oregon: Portland, Ore., Portland State University, M.S. thesis*, 82 p.
- Long, P. E., and Duncan, R. A., 1982, $^{40}\text{Ar}/^{39}\text{Ar}$ ages of Columbia River Basalt from deep boreholes south Central Washington [abs]: *Alaska Science Conference, 33rd, Fairbanks, Alaska, Proceedings*, p. 119.
- Madin, I. P., 1990, *Earthquake-hazard geology maps of the Portland metropolitan area: Oregon Department of Geology and Mineral Industries Open-File Report O-90-2*, 21 p, scale 1:24,000.
- Madin, I. P., 1994, *Geologic map of the Damascus quadrangle, Clackamas and Multnomah counties, Oregon: Oregon Department of Geology and Mineral Industries Geological Map Series 60*.
- Madin, I. P., 2004, *Geologic mapping and database for Portland area fault studies, final technical report: Oregon Department of Geology and Mineral Industries Open-File Report O-04-2*, 18 p.
- Palmer, A. R., and Geissman, J., 1999, 1999 *Geologic time scale: Boulder Colo., Geological Society of America*, 1 p.

- Reidel, S. P., 2005, A lava flow without a source: The Cohasset Flow and its compositional components, Sentinel Bluffs Member, Columbia River Basalt Group: *Journal of Geology*, v. 113, p. 1–21.
- Reidel, S. P., Tolan, T. L., Hooper, P. R., Beeson, M. H., Fecht, K. R., Bentley, R. D., and Anderson, J. L., 1989, The Grande Ronde Basalt, Columbia River Basalt Group; Stratigraphic descriptions and correlations in Washington, Oregon, and Idaho, *in* Reidel, S. P., and Hooper, P. R., eds., *Volcanism and tectonism in the Columbia River Flood-Basalt Province*: Geological Society of America Special Paper 239, p. 21–53.
- Schlicker, H. G., and Finlayson, C. T., 1979, Geology and geologic hazards of northwest Clackamas County, Oregon: Oregon Department of Geology and Mineral Industries Bulletin 99, 79 p., 10 plates.
- Swanson, D. A., Wright, T. L., Hooper, P. R., and Bentley, R. D., 1979, Revisions in stratigraphic nomenclature of the Columbia River Basalt Group: U.S. Geological Survey Bulletin 1457-G, 59 p.
- Tolan, T. L., Reidel, S. P., Beeson, M. H., Anderson, J. L., Fecht, K. R., and Swanson, D. A., 1989, Revisions to the estimates of the areal extent and volume of the Columbia River Basalt Group, *in* Reidel, S. P., and Hooper, P. R., eds., *Volcanism and tectonism in the Columbia River Flood-Basalt Province*: Geological Society of America Special Paper 239, p. 1–20.
- Treasher, R. C., 1942, Geologic history of the Portland area: Oregon Department of Geology and Mineral Industries Short Paper 7, 17 p., 1 pl.
- Trimble, D. E., 1963, Geology of Portland, Oregon, and adjacent areas: U.S. Geological Survey Bulletin 1119, 119 p.
- U.S. Geological Survey, 2006, Columbia River Basalt stratigraphy in Oregon. http://or.water.usgs.gov/proj_dir/crbg/, accessed October 6, 2006.
- Waite, R. B., 1985, Case for periodic, colossal jokulhlaups from Pleistocene glacial Lake Missoula: Geological Society of America Bulletin, v. 96, no. 10, p. 1271–1286.